

**A NATIONAL MEASUREMENT
GOOD PRACTICE GUIDE**

No. 12

Biaxial Flexural
Strength Testing of
Ceramic Materials

Measurement Good Practice Guide No. 12

Biaxial Flexural Strength Testing of Ceramic Materials

Roger Morrell

Centre for Materials Measurement and Technology
National Physical Laboratory

Abstract: This guide is intended to act as a review of mechanical testing of disc-shaped test-pieces of ceramic materials, as commonly encountered in substrates, windows and membranes, and in materials research in which discs are the simplest form of test-piece that can be produced. Unlike uniaxial testing of beams in flexure, there are numerous issues concerning the accuracy of analytical equations, frictional errors, alignment, conformance of loading contacts, and large deflections producing membrane stresses. This guide reviews the options for undertaking biaxial testing, very few procedures for which have reached the stage of formal standardisation. This guide will have value to those considering undertaking biaxial testing in providing information on test-jig design, potential inaccuracies, and interpretation of test results.

© Crown Copyright 1998
Reproduced with the permission of the Controller of HMSO
and Queen's Printer for Scotland

ISSN 1368-6550

September 1998
(reviewed and updated December 2007)

National Physical Laboratory
Teddington, Middlesex, UK, TW11 0LW

Acknowledgements

This guide has been produced in a *Characterisation of Advanced Materials* project, part of the *Materials Measurement* programme sponsored by the Engineering Industries Directorate of the Department of Trade and Industry. The advice and steer from the Ceramics and Hardmetals Industrial Advisory Group in reviewing the Guide are gratefully acknowledged.

The author would also like to acknowledge collaborations with Jim Margetson of the Defence Research Consultancy concerning finite element analysis, and with George D. Quinn of the Ceramics Division, National Institute of Standards and Technology, Gaithersburg, Maryland, USA, and formerly of US Army Materials Laboratory, Watertown, Mass., USA, concerning technical assessments. Several NPL colleagues are also thanked: Maria Lodeiro and Jonathan Bevan for work on large strain-gauged discs, John Cox and Liam Byrne for test-jig design and operation experience, Dave Ferriss for verifying the ring-on-ring equations, and Lewis Lay and Bryan Roebuck for reviewing the manuscript and offering helpful suggestions.

For further information on *Materials Measurement* contact the Materials Enquiry Point at the National Physical Laboratory:

Tel: 020 8943 6701
Fax: 020 8943 7160
E-mail: materials@npl.co.uk

Biaxial Flexural Strength Testing of Ceramic Materials

Contents

Executive summary

List of symbols

1.	Introduction	1
2.	General discussion of test geometry	5
	2.1 Introduction	5
	2.2 Ring supported/ring loaded geometry	7
	2.3 Ring supported/ball loaded geometry	8
	2.4 Three-ball support/piston loaded.....	8
	2.5 Square plate tests.....	9
	2.6 Discussion	9
3.	Test-jig design	12
	3.1 Ring supported/ring loaded geometry	12
	3.2 Three-ball support geometry	16
	3.3 Square plate test jigs	16
4.	Test-piece preparation	17
	4.1 Dimensions.....	17
	4.2 Edge finish.....	17
	4.3 Surface finish.....	18
	4.4 Dimensional tolerances.....	18
	4.5 Number of test-pieces	19
5.	Test procedure	19
	5.1 Measuring test-piece and test-jig dimensions	19
	5.2 Assembling test-piece and test jig	20
	5.3 Conducting the test.....	20
	5.4 Calculating strength	21
	5.5 Undertaking fractography	21
6	Comparison of biaxial and uniaxial strengths	23

7	Use of biaxial testing for subcritical crack growth and fracture toughness tests	24
8	Tests at raised temperatures	24
9	Conclusions	25
10.	Bibliography	26
Annex A – Determination of elastic properties using the impact excitation method		
	on disc test-pieces	29
A.1	Introduction	29
A.2	Disc vibration modes and test principle	29
A.3	Test method	29
A.4	Experimental technique	31
A.5	Limitations.....	32
A.6	Bibliography.....	33
Annex B – Large deflection analysis for thin discs		
B.1	Introduction	36
B.2	Analysis	36
B.3	Conclusions	37
B.4	Bibliography.....	38
Annex C – Stress analysis and the role of friction in the ring supported/ring loaded geometry.....		
C.1	Introduction	41
C.2	Stress concentrations.....	41
C.3	Friction	42
	C.3.1 Analytical approach	42
	C.3.2 2D finite element analysis (FEA)	42
	C.3.3 3D FEA.....	46
C.4	Alignment.....	46
C.5	Bibliography.....	48
Annex D – Bibliography on biaxial testing of ceramics and glass		
D.1	Introduction	49
D.2	Bibliography.....	49

Executive summary

This Good Practice Guide provides an overview of biaxial flexural strength testing of ceramic materials. Biaxial testing has been claimed to be more searching of strength limitations in brittle materials by testing a larger volume than in beam flexure. Disc or square test-pieces are easier to prepare, especially under laboratory conditions, than bar test-pieces, and require less machining. In addition, edge preparation is less critical because maximum stresses applied are remote from edges. Against these potential testing advantages are some distinct disadvantages. In contrast with the well researched and understood bar flexural strength test which has led to clearly defined standards, biaxial testing appears to be rather more difficult to perform well. A very wide range of test geometries has been used, and all have some uncertainties associated with them in terms of assumptions in the derivation of equations for stress and potential experimental errors.

This guide reviews the technical literature and assesses the problems associated with the various test geometries, including:

- ring supported, ring or flatted-ball loaded
- ring-of-balls supported, ring-of-balls loaded
- three ball supported, punch, ball, or flatted-ball loaded
- ring supported, pressurised.

Test-jig design is covered, with particular note being made of methods of overcoming friction and enabling the supporting and loading contacts to conform to the test-piece surfaces. Recommendations are made for good practice concerning test-piece preparation, conducting the test, and fractographic analysis of the site of fracture. Annexes deal with:

- accurately determining Poisson's ratio, a parameter required in all equations for calculating fracture stress, from disc test-pieces;
- analysis for thin test-pieces when large deflections are obtained, because the load/ stress relationship is no longer linear and numerical solutions are needed to determine fracture stress;
- analyses of potential errors incurred in assuming the absence of friction, 'thin' test-pieces, and perfect axial alignment of test-piece and test-jig parts.

The Guide is appropriate for those characterising ceramic and other brittle materials who wish to embark on biaxial testing by introducing the topic, enabling options to be identified, and providing a gateway to the literature on the subject.

List of symbols

a	support ring radius
b	load ring radius
b'	ball contact area radius
\bar{b}	equivalent radius of contact of ball
d	diameter of disc
d_b	diameter of ball
E	Young's modulus
E_b	Young's modulus of ball
E_c	Young's modulus of ceramic test-piece
f_1	frequency of first ('saddle') mode of vibration of test-piece
f_2	frequency of second ('diaphragm') mode of vibration of test-piece
F	force applied to test-piece
G	shear modulus
K_1	constant for first mode of vibration
K_2	constant for second mode of vibration
m	mass of test-piece
p	pressure applied to test-piece
r	radius variable in test-piece
R	radius of test-piece
t	thickness of test-piece
w_0	central deflection in test-piece
ε_f	strain at fracture
θ	angle variable
μ	friction coefficient
ν	Poisson's ratio
ν_b	Poisson's ratio of ball
ν_c	Poisson's ratio of ceramic test-piece
σ	stress
σ_0	stress due to applied pressure
σ_f	fracture stress
σ_r	radial stress
σ_θ	tangential stress

1. Introduction

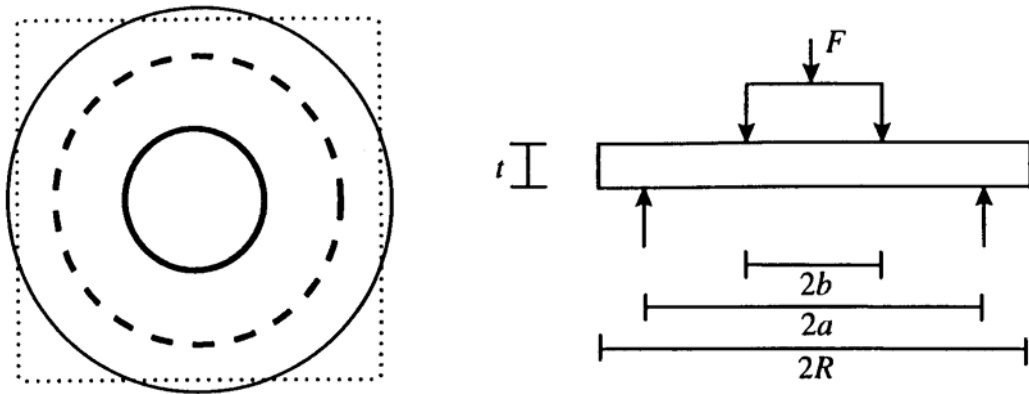
Testing of disc-shaped test-pieces in flexure is a popular method of determining strength, especially for materials produced as thin flat sheet, or for research purposes in which pressed discs are one of the most readily produced shapes. However, disc testing has not received the same level of critical review and optimisation as flexural testing of bar test-pieces. There are few standards, and there appear to remain many uncertainties. Best practices are therefore poorly understood, and potential sources of error have not been properly identified and assessed.

There are many methods of undertaking disc flexural testing described in the scientific and technical literature, and they have different potential advantages and disadvantages. Figure 1 and Table 1 summarise the range of geometries. They fall into two main categories; those which are circularly symmetrical in the stress field developed, and those which are not, as a result of a different symmetry in the method of loading. Normally, in each case the stress at failure is calculated from thin plate flexure theory, usually assuming that failure initiates within the zone of highest stress which is typically equibiaxial, or near equibiaxial (see Table 1). Few of these methods have been formally standardised.

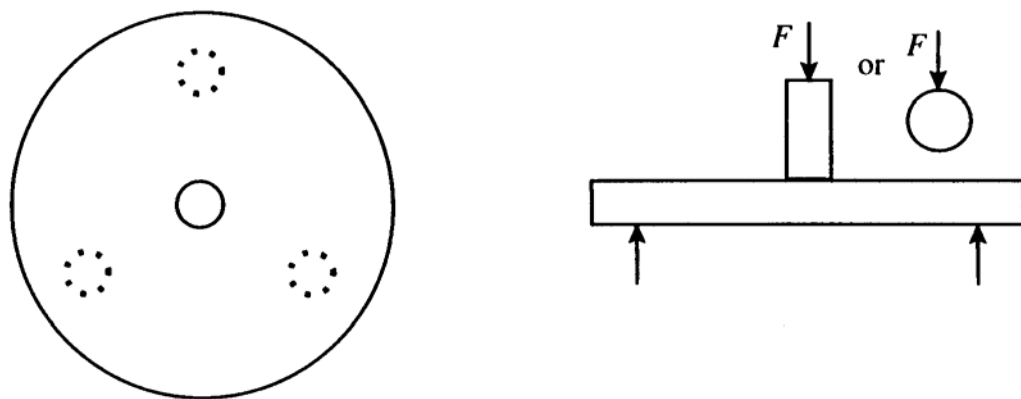
Without exception, calculation of fracture stress requires the assumption of, or prior knowledge of, Poisson's ratio. This may not be known for the material under test. Annex A gives a method of determining elastic moduli, including Poisson's ratio, on disc test-pieces by use of the so-called impact excitation method. This is not the only method, of course, but is convenient for discs of reasonable size. Alternative methods include strain gauging the central region under uniform stress and displacement methods during flexure, either measuring displacements mechanically or by indirect means such as laser speckle interferometry (*e.g.* Furguiele *et al.* (1995)).

This review and Guide describes the variety of test methods available, reviews the advantages and disadvantages of each, and attempts to identify the currently most appropriate methods for general use. Potential errors are assessed where possible. The document cannot be considered to be complete in every respect because the required research has not been carried out, but it is hoped that the reader will gain a better understanding of the factors of importance in selecting and undertaking a test.

Ring supported/ring loaded disc or square



Three-ball supported/ram or ball loaded:



Ring-supported /pressure loaded disc:

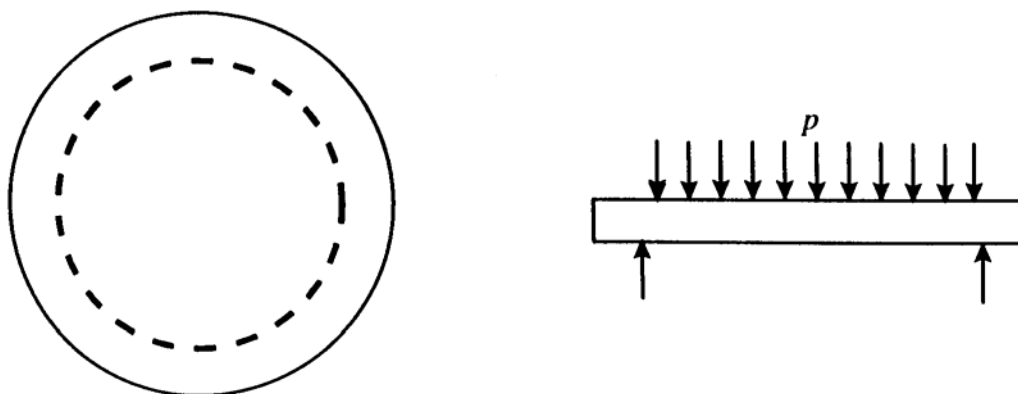


Figure 1 - Various geometries for disc testing.

Table 1 – Test geometries and analytical equations

Geometry	Sources	Equations for maximum stress
Ring supported/ring loaded (included in ISO 6474 and ISO 13356)	Vitman and Pukh (1963) Ritter <i>et al.</i> (1980) Fessler and Fricker (1984) Soltész <i>et al.</i> (1987)	$\sigma_r = \sigma_t = \frac{3(1+\nu)P}{2\pi t^2} \left[\ln \frac{a}{b} + \frac{(1-\nu)(a^2 - b^2)}{(1+\nu)2R^2} \right]$
Three ball support/piston loaded (ASTM F394) Three ball support/ball with flat loaded	Kirstein and Woolley (1967) Wachtman <i>et al.</i> (1972)	$\sigma_t = \sigma_r = \frac{3(1+\nu)P}{4\pi t^2} \left[1 + 2 \ln \frac{a}{b} + \frac{(1-\nu)}{(2+\nu)} \left(1 - \frac{b^2}{2a^2} \right) \frac{a^2}{R^2} \right]$
Ring supported/ ball loaded	Shetty <i>et al.</i> (1980)	As piston on three balls, but with approximation of ball contact radius $b' \approx 0.1t$ and an "equivalent radius of contact" $b \approx t/3$
Ring supported/ ball with flat loaded	Wilshaw (1968)	As ring supported/ring loaded.
Three ball support/ ball loaded	Godfrey (1985) Roark and Young (1975)	As piston on three balls, but assuming radius of contact b' is given by Hertzian flattening of loading ball on a flat surface: $b' = 0.721 \left[Pd_b \left(\frac{(1-\nu_b^2)}{E_b} + \frac{(1-\nu_c^2)}{E_c} \right) \right]^{1/3}$

Table 1 (cont.) – Test geometries and analytical equations

Geometry	Sources	Equations for maximum stress
Corner-supported square plate, ring loaded	Entwhistle (1995)	Finite element analysis leading to tabular calibration for two ring diameter to plate side length geometries, see original reference
Pressurised circular plate	Matthewson and Field (1980) Shetty <i>et al.</i> (1983) Timoshenko <i>et al.</i> (1959) Newton <i>et al.</i> (1995)	<p>Assuming uniform pressure over entire plate area:</p> $\sigma_r = \frac{3pa^2}{8f^2} \left[2(1-\nu) + (1-3\nu) \left(\frac{R^2}{a^2} \right) - 4(1-\nu) \left(\frac{R^2}{a^2} \right) \ln \left(\frac{R}{a} \right) - (3+\nu) \left(\frac{r}{a} \right)^2 \right] + \sigma_0$ $\sigma_\theta = \frac{3pa^2}{8f^2} \left[2(1-\nu) + (1-3\nu) \left(\frac{R^2}{a^2} \right) - 4(1-\nu) \left(\frac{R^2}{a^2} \right) \ln \left(\frac{R}{a} \right) - (1+3\nu) \left(\frac{r}{a} \right)^2 \right] + \sigma_0$ $\sigma_0 = [(3+\nu)p / 4(1-\nu)]$

2. General discussion of test geometry

2.1 Introduction

In biaxial flexural testing the test-piece has to be supported in some way and bent by a means of applying forces to its surfaces. The various ways of doing this are summarised in Table 1 and shown schematically in Figure 1. Typically the disc or square plate test-piece is supported near its periphery and is loaded by a coaxially located ball, punch, or ring, or is pressurised. In the circularly symmetrical and locally loaded geometries, the stress field is equibiaxial in the central region in which it is a maximum. In the non-circular, or circular, but point supported cases, the stress field depends on the position between the supports, but can approximate to equibiaxial away from the supports. In the case of a pressurised disc, the stress field is equibiaxial only at the disc centre.

In each of the geometries, therefore, the stress field is different and requires different calculation equations, and some of them do not have convenient analytical solutions for the stress distribution. The advantages and disadvantages of each geometry are summarised in Table 2, and are discussed briefly below and in more detail in the Annexes. It should be noted that there are a number of assumptions made in the simple analytical theory of plate bending, such as ignoring frictional effects at contact points, and validity for small deflections only (usually rather less than the plate thickness).

The extent of overhang of the test-piece outside the support ring is also important. This region has the effect of providing strong support for the test-piece during loading, and also stiffens the test-piece against deflection in the central region. This stiffening must be accounted for in the calculation of stress.

The mechanical analysis of any of the test geometries usually relies on some simple assumptions, typically that the deflection is at all times small compared with the thickness of the disc, and that no friction is present at contacting surfaces:

- In the case of deflections larger than about one-half of the test-piece thickness the force/displacement and force/stress relationships are no longer linear. This greatly increases the complexity of the analysis. The topic is discussed at greater length in Annex B, but it is highly desirable to operate, where possible, within the linear elastic region, which is when the support radius to disc thickness ratio is less than about 20 to 50, depending on the strain to fracture.

Table 2 – Summary of advantages and disadvantages of geometrical types

Test type	Advantages	Disadvantages
Ring supported/ ring loaded	Symmetrical and approximately constant equibiaxial stress inside loading ring	Requires flat test-pieces (slight out-of-flatness may be removed by using rubber sheet or compliant rings) Friction effects difficult to control
Ring supported/ ball loaded	Symmetrical Self-aligning	Requires flat test-pieces Very limited volume under stress Assumptions about contact area between ball and test-piece
Ring supported/ ball-with-flat loaded	Symmetrical Self-aligning	Requires flat test-pieces
Three-ball support/ piston loaded	Copes with out-of-flatness of test-piece	Very limited volume under stress Possible misalignment of test-piece relative to piston end Friction effects unknown
Three-ball support/ ball loaded	Copes with out-of-flatness of test-piece	Very limited volume under stress Assumptions about contact area between ball and test-piece
Three-ball support/ ball-with-flat loaded	Copes with some out-of-flatness of test-piece Defined loaded area	Validity of three-ball support/piston loaded equation uncertain (not locally pressurised, but ring loaded)
Ring-of-balls support/ ball loaded	Potential for reducing friction if balls can roll freely	Requires flat test-pieces Assumptions about contact area between ball and test-piece
Ring-of-balls support/ ring-of-balls loaded	Potential for reducing friction if balls can roll freely	Requires flat test-pieces
Ring supported/ pressure loaded	Can cope with out-of-flatness if compliant support used	Requires expensive test jig Slow to set up for each test
Four ball support/ ring loaded	Ideal for square test-pieces Frictionless contact at supports	Requires flat test-piece No analytical solution available

- In the case of friction at test-piece supports, this can have a major effect on the stress distribution, especially for thicker discs. Some information on the effects of friction will be found in Annex C. Ignoring friction will lead to systematic overestimation of strength by a few percent for disc support radius to thickness ratios of typically 20, up to tens of percent for support radius to thickness ratios of less than 5. Friction can be minimised by using compliant layers which permit shear across the support points, or by devising rolling support points as in beam flexure tests.

2.2 Ring supported/ring loaded geometry

This is the simplest symmetrical form of loading, an analogue of four-point flexure on bars, and is usually achieved by use of round or semicircular cross-section rings positioned concentrically on the test-piece. The ratio of the ring centre diameters is not critical, but is typically between 4:1 and 2:1. If the loading rings are made of a rigid material such as steel, they are not compliant and do not follow slight out-of-flatness of the test-piece. It is recommended by Soltész *et al.* (1987) that thin rubber sheet, typically 1 mm thick, is used between the test-piece and the support ring to accommodate this. Between the loading ring and the test-piece, paper is recommended. These recommendations have been incorporated into ISO 6474 (alumina ceramics for surgery) and ISO 13356 (zirconia ceramics for surgery), which use 36 mm diameter test-pieces supported on a 30 mm diameter ring and loaded by a 12 mm diameter ring.

A potential advantage of the rubber sheet is that it permits some shear, and thus may help to reduce frictional effects. Attempts at NPL to verify this using a large strain gauged test-piece have not given results consistent enough to prove its effectiveness.

The equation for calculating the equibiaxial stress in the central region (see Table 1) assumes that the disc is thin compared with its diameter, has only a small deflection, and gives zero friction at load contacts. However, more-detailed analyses (Fessler and Fricker (1984), Morrell *et al.* (1998)) show that if such assumptions are not valid, large errors can arise. Moreover, finite element analysis shows that there is a small peak in radial tensile stress opposite the loading ring, which helps to explain the frequently observed tendency for fracture to originate from near the loading ring position. This stress concentration worsens as the disc thickness increases, or for thin discs, as the deflection increases. This test has also been used with square test-pieces. In this case, the stress field is perturbed a little by the additional stiffness of the overhang region, but it has been shown that if the average overhang is taken, the error in calculating the maximum nominal stress inside the loading ring is negligible.

Godfrey and John (1986) have proposed the replacement of the support and loading rings by rings of captive balls on the grounds that uniform sized balls are easier to obtain and to replace when damaged than solid rings. Using reaction bonded silicon nitride discs as the test material, they showed that a test jig incorporating twelve 1 mm balls as the support ring gave very similar results to those obtained using solid rings.

2.3 Ring supported/ball loaded geometry

This is the analogue of three-point flexure of a bar test-piece, but compared with the ring supported/ring loaded geometry has some disadvantages. It will be noted that the term $\ln(a/b)$ in the stress formula for the ring/ring geometry becomes large and essentially indeterminate as the loading ring radius, b , becomes very small, as applies in ball loading. There is a need to make some assumptions as to what happens under the loading ball. It is usually assumed that Hertzian flattening of the ball leads to a contact area under which there is a contact pressure distribution, and this gives rise to high equibiaxial tensile stresses on the opposite surface immediately under the ball. The maximum stress is thus highly localised. Only a small volume or surface area of test-piece is subjected to the maximum stress compared with the ring/ring case, and the contact area is a function of applied force. Such features are often considered to be disadvantageous in ceramic testing particularly for design extrapolation purposes.

One method of spreading the load over a larger area is to place a small flat on the loading ball (Wilshaw (1968)). This has the advantage of defining the radius of contact, and once the disc has deflected a little, essentially becomes ring on ring geometry again.

2.4 Three-ball support/piston loaded

This test was developed primarily to overcome out-of-flatness of test-pieces, which will always locate readily on three points. The loading method proposed originally by Wachtman *et al.* (1972), following a stress analysis by Kirstein and Woolley (1967), has become standardised in ASTM F394 for testing electronic substrate materials. In the standard, a disc of about 32 mm diameter is supported on three 3.2 mm diameter balls equally spaced on a 25.4 mm diameter circle, and is centrally loaded by a guided punch of 1.6 mm diameter. A load spreader such as 0.05 mm polyethylene sheet is used under the punch to take out misalignments and lack of flatness. This method has the advantage that it is very simple practically, but has uncertainties concerning the exact stress distribution over the very small region under the piston end. Using a guided piston rather than a self-aligning contact, there is always the risk of misalignment, and damage can occur to the piston tip during fracture.

A modification to this suggested by Godfrey (1985) is to use a large diameter ball instead of a punch, and to compute the contact radius from Hertzian flattening. As with the ball on ring test described above, the area of contact is a strong function of load, which means that the volume or surface area under stress at failure will vary from test-piece to test-piece. However, the system is inherently self-centring and self-aligning, which is an experimental advantage.

Again, as with the ring supported ball loaded case, the contact area can be defined by placing a small flat on the loading ball. The same equation can be used provided that it is assumed that

there is uniform pressure under the flattened region, achieved by using a load spreader as in the piston test. This method was used in an unpublished round robin exercise (Morrell (1988)), but because the test material proved to have a bimodal strength distribution, consistency of results was difficult to prove.

2.5 Square plate tests

As mentioned above, if a square plate is tested using the ring supported/ring loaded geometry, an equivalent 'radius' of the test-piece is empirically one-half of the sum of the edge and diagonal lengths (equal to 1.207 times the side length, Vitman and Pukh (1963)), permitting the disc equations for the ring/ring geometry to be employed. Ritter *et al.* (1980) have confirmed by finite element analysis that the stress distribution in the central region is virtually independent of whether the overhang region is square or circular, although clearly there are differences outside the loading ring diameter. The risk of failure from such regions is small, and thus the test should be applicable equally to square test-pieces as to discs.

Entwhistle (1995) has proposed an alternative method of support using four balls symmetrically positioned in vee-grooves aligned with the diagonals of the square test-piece. Loading is via a centrally positioned neoprene O-ring. Support near the corners of the plate leads to high stresses midway along the plate edges, but moving the support points closer towards the plate centre reduces the risk of edge failure. A finite element analysis (FEA) has been performed for the case of thin plates with deflections typical of the plate thickness. This showed a good correlation with measured displacements, and has been used to identify recommended geometries in which the behaviour is linear to fracture, specifically that the diameter of the support ball circle should be 0.85 of the side length of the square test-piece, and the loading rings should have diameters of 0.25 and 0.075 of the side length of the square test-piece. This arrangement has the clear advantage of minimising frictional forces at the support balls since they are free to move in the vee-grooves.

2.6 Discussion

It will be clear to the reader that each of the test methods has its own advantages and disadvantages, summarised in Table 2, in terms of giving reliable behaviour in accordance with simple analytical expressions for small deflections. There does not seem to be an optimum choice. It is currently considered that there are significant uncertainties associated with all the methods, which might easily lead to stress errors of 10% or more, depending on the precision of the test-piece, the test jig function, the interfacial contacts, and the simplifying assumptions made in the stress analysis. Furthermore, it is likely that each method will have different effective stressed volumes or surface areas, and thus will give different results when used on the same material. As far as the author is aware, only a small number of instances of such comparative work are available in the scientific literature to permit proper comparative evaluations. Round

robin exercises, such as those reported by Wachtman *et al.* (1972) and Morrell (1988), show that a given technique can give reasonably reproducible results between laboratories, but these studies are not especially helpful in identifying where the fundamental error problems lie.

Figure 2 shows a flow chart which may be helpful for the selection of a test method, based on three main criteria:

- whether square or circular test-pieces are to be used;
- whether they are sufficiently flat that any out-of-flatness can be absorbed by the test jig without significant influence on the stress distribution achieved;
- whether the data are required purely for historical comparison purposes or are needed for engineering design extrapolation requiring accuracy of strength determination.

A secondary criterion is the expected degree of deflection of the test-piece at fracture. If this exceeds the plate thickness the simple thin-plate analysis is not valid, and corrections need to be employed (see Annex B). These corrections are reasonably well known only for the circularly symmetrical system with ring support/ring loading, and by implication above, can probably be reasonably extrapolated to square test-pieces with the same loading configuration. However, the less well-defined loading systems may not have suitable large deflection analyses.

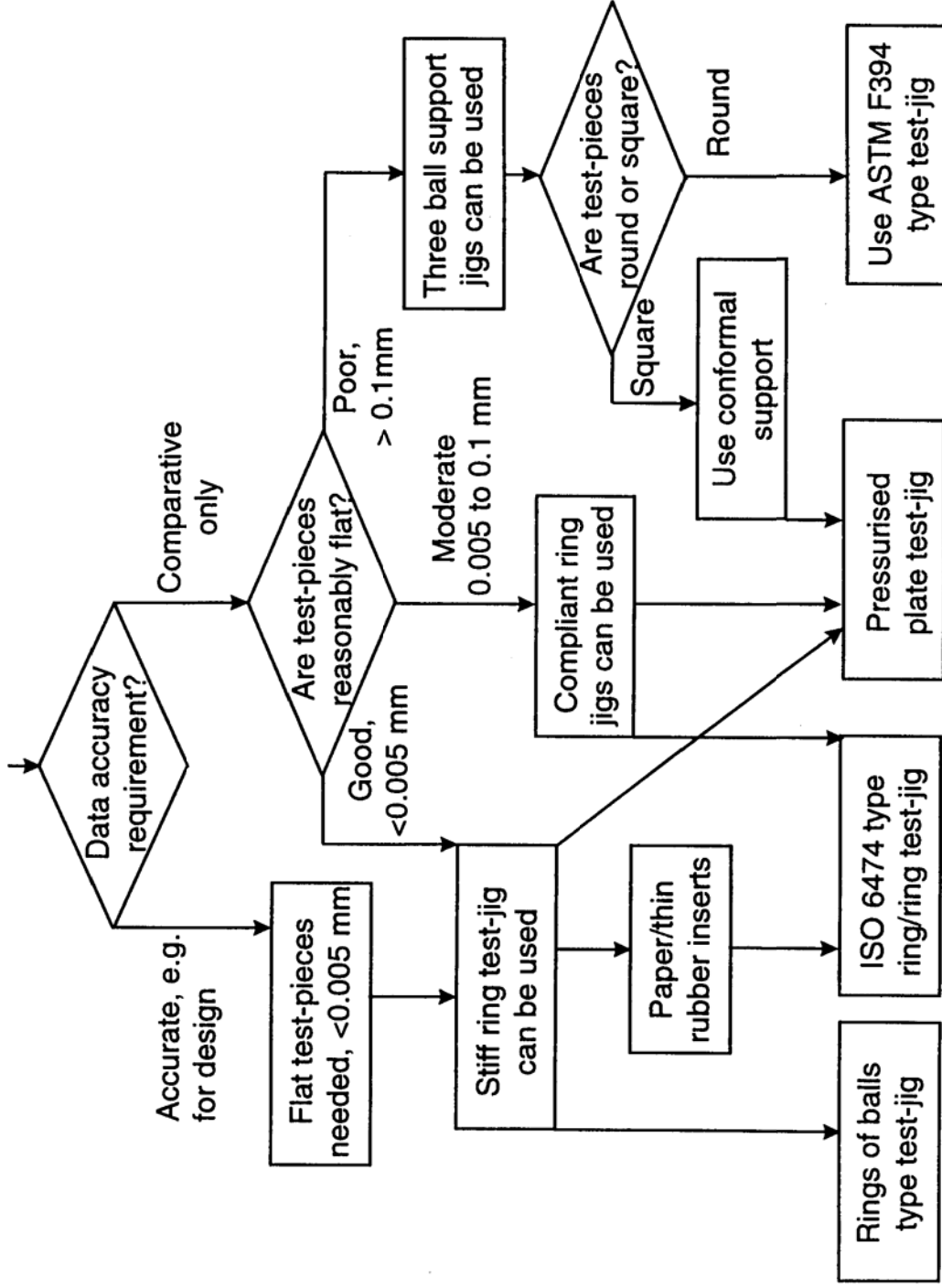


Figure 2 - Flow chart for selection of test method. The out-of-flatness figures are thought to be appropriate for test-pieces 20-40 mm diameter with diameter to thickness ratios of between 20 and 100. Larger figures would be appropriate for larger diameters or thinner test-pieces.

3. Test-jig design

3.1 Ring supported/ring loaded geometry

The simplest way of defining the support and loading circle contacts is by using well-defined toroidal or semi-toroidal sections in appropriate materials (Figure 3(a), 3(b)). Using a hard surface, *e.g.* steel, gives little if any compliance to take up out-of-flatness of the test-piece, but this can be compensated for by using rubber sheet between the test-piece and the ring as in ISO 6474. This also has the advantage of possibly reducing friction at lines of contact. In the vast majority of examples in the literature such hard rounded rings are employed. However, alternatively, compliant materials, such as neoprene or other relatively hard, elastic polymers have also been successfully used (*e.g.* Adler and Mihora (1992)). Finite element analysis has shown that compliant rings, even with rectangular (Figure 3(c)) rather than round cross-sections, although they do not define the support dimension as accurately as hard rounded rings, do not have associated with them the stress concentration effects produced by hard rings (see Annex C). Soft rings can probably be used for slightly out-of-flat test-pieces, but run the risk of becoming damaged more readily when the test-piece fractures. More frequent replacement can be envisaged than with harder metal rings, although even these need to be re-polished from time to time.

Hard ring surfaces need to be polished to minimise friction, but because a toroid cannot roll in the same way as a roller in a beam test, some frictional element will still exist. Whether friction is sensibly reduced or eliminated by using soft loading rings which can deform is unclear. Replacing the solid rings by rings of balls has been tried (Shetty *et al.* (1980), Godfrey and John (1986), Figure 4). This is a cost-effective solution, because ball bearings of uniform size are readily available and easy to replace. However, there remains a question as to whether balls convey any advantage in being able to eliminate friction by rolling in the correct way, because simple designs keep the balls captive in a ball race or in a groove which would permit only free tangential rolling, not radial. Ideally, to ensure elimination of friction, the balls need to rest in individual radial vee-grooves, as proposed by Entwistle (1991) for the square plate test (section 3.3). Furgiuele *et al.* (1997) report using 36 radial grooves for the support ball system for the pressurised disc method, but such an arrangement has not been reported for conventional ring/ring testing as far as can be ascertained. Restraining the balls in the starting position, especially in the upper loading unit, would require some ingenuity.

Other alternatives to continuous rings have been tried. Evans and Davidge (1971) employed a segmented support ring in which each segment was allowed to float on a compliant spring at low applied force to take up out-of flatness of moulded glass test-pieces. The segments were then clamped at the correct heights for each test-piece, and the test resumed to fracture. This requires individual attention to each test-piece. Noting the problem, Marshall (1980) designed

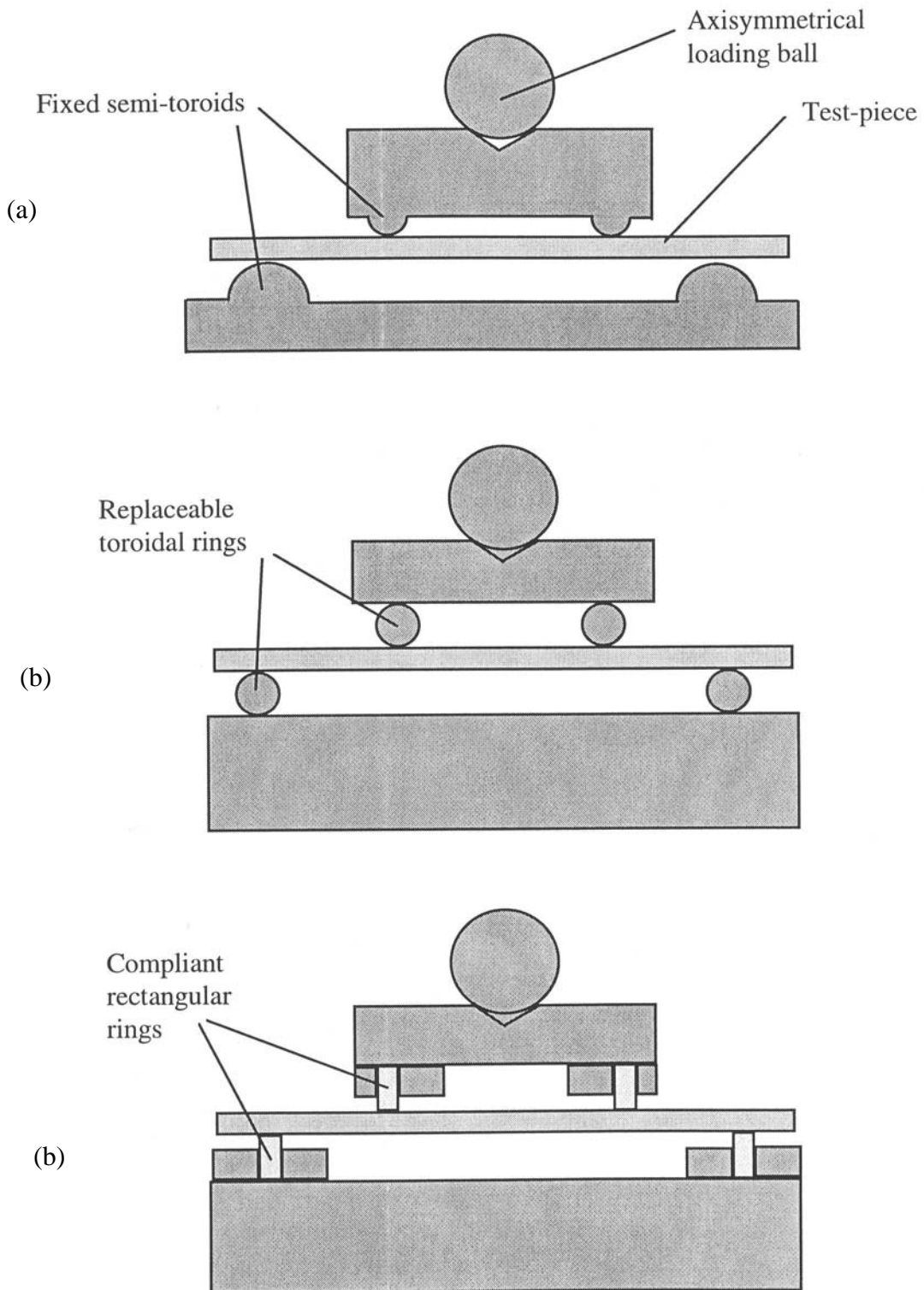


Figure 3 - Loading methods for the ring-on-ring geometry using (a) solid semi-toroids, (b) replaceable toroids, and (c) replaceable rectangular section rings.

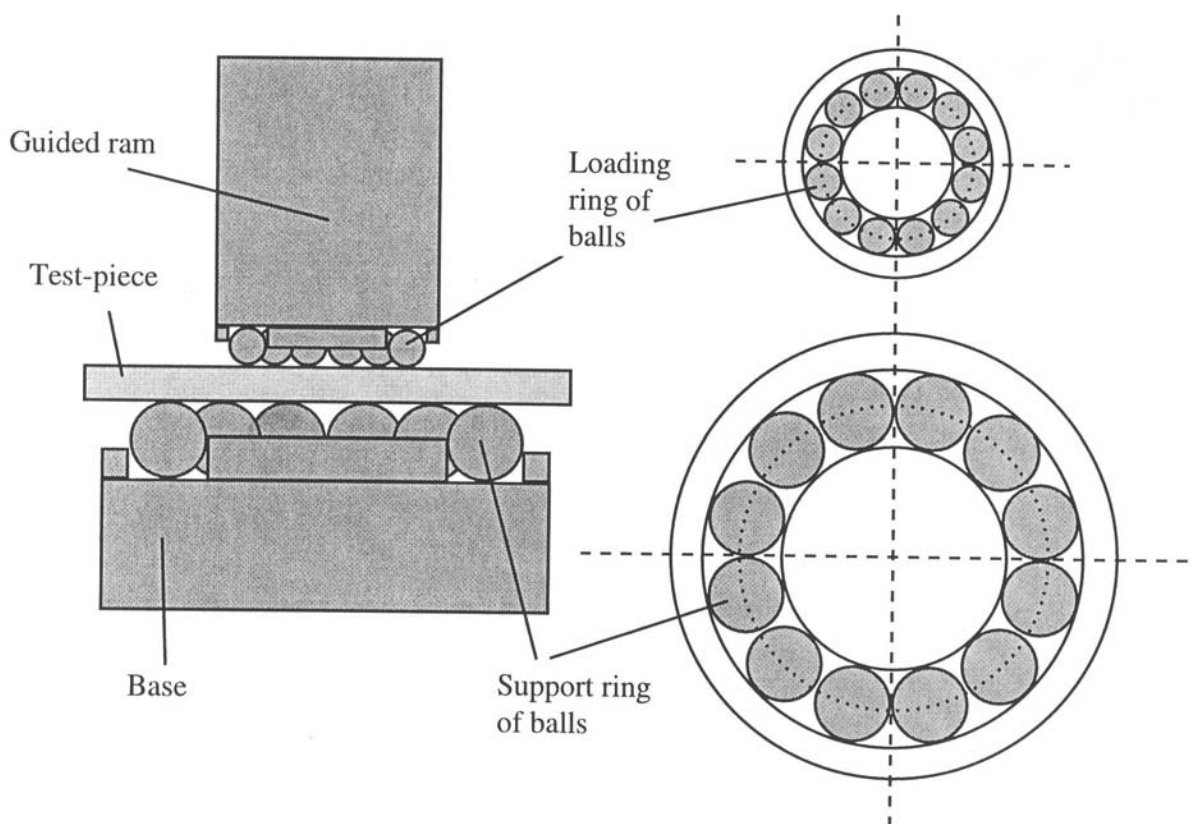


Figure 4 - A test jig design employing rings of balls (after Godfrey and John (1986)).

the rings to be made from closely wound, helically coiled wire supported on a liquid-filled rubber diaphragm. In this way they essentially float to take up out-of flatness in the test-piece. The system also has the advantage of providing an indicator of lack of coaxiality, which tilts the test-piece. Its disadvantage is said to be its non-linear compliance on loading. This can be reduced by inserting a more-compliant element in the loading system, permitting constant displacement rate testing to be used. Strain gauge evaluation of the stress distribution in the test-piece showed that it was a significant improvement over the rigid loading ring system. A similar approach has been reported by Manley *et al.* (1994) who employed teflon O-rings supported on liquid-filled diaphragms (Figure 5).

The support and loading rings need to be coaxial to quite high precision. It has been demonstrated (Morrell *et al.* (1998)) that failure to align with a precision of better than 2% of the disc diameter can incur errors in the maximum stress of typically 10%, increasing with reducing test-piece thickness (for more details see Annex C). Since the two rings need to float

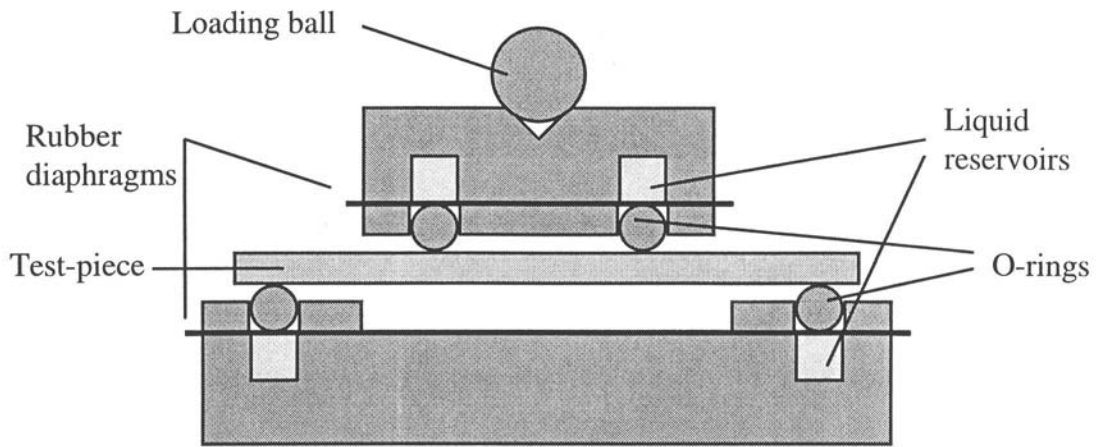


Figure 5 - Schematic of the liquid-filled diaphragm ring/ring design proposed by Marshall (1980) and Manley et al. (1994).

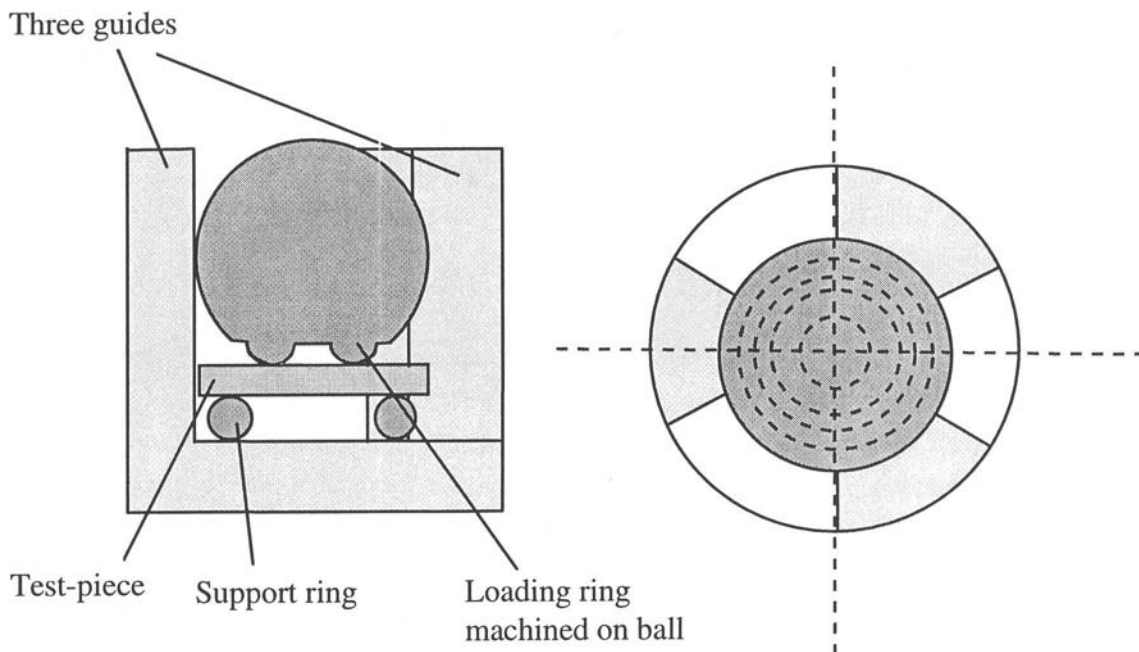


Figure 6 - Schematic of a ring supported/ring loaded test jig based on a large ball which permits articulation of the loading ring and reasonable centring relative to the support ring.

freely and possibly to articulate relative to each other, a guidance system is required to ensure alignment. Fessler and Fricker (1984) machined the loading ring on a large ball which slid in a guide coaxial with the support ring (Figure 6). A similar design was used by Godfrey (1985) for direct ball loading and for a UK round robin using three-ball support and ball with a flat loading (Morrell (1988), see below). This has the advantage of easy articulation compared with guided piston arrangements (*e.g.* Godfrey and John (1986)).

3.2 Three-ball support geometry

In the ASTM F394 recommended design, three captive steel balls are positioned symmetrically on a 25.4 mm diameter circle, with no requirement that the balls should be capable of rotation. The loading piston is guided to run normally to the mounting plane of the support balls through low-friction precision linear ball races, and its tip comprises a hardened steel cylinder with a 1.6 mm diameter. It must be centred relative to the centre of the support ball circle to within 0.8 mm. This arrangement does not permit articulation of the loading tip to accommodate jig machining tolerances or out-of-flatness of the test-piece, which can induce errors in the stress distribution achieved in the test-piece. A load spreader comprising 0.05 mm thick polyethylene is recommended between the loading piston end and the test-piece, which is thought to be adequate for most circumstances, but it is difficult to prove that it is truly effective in equalising the pressure under the loading tip.

In order to improve the alignment, a large ball bearing can be used sliding in a guide, similar to that shown in Figure 6. Godfrey (1985) used the ball directly and calculated the radius of Hertzian flattening, which is a function of applied force. The disadvantages of this approach are the assumptions that the test-piece remains flat and that the elastic properties of the ball and the test-piece are previously known. Placing a small flat on the ball helps to define the contact radius. Whichever method is used, the contact radius should be kept small compared with the support circle diameter to ensure that the ASTM F394 equations are still valid.

The concept introduced by Entwistle (1991) of supporting the balls in radial vee-grooves to essentially eliminate friction effects has not been reported for the three ball support test geometry.

3.3 Square plate test jigs

Entwistle (1991) used a design in which four support balls are positioned symmetrically in two orthogonal vee-grooves. He used 9.5 mm balls for testing 103 mm square alumina ceramic substrates, with the balls initially positioned at the corners of the substrate. In later work (Entwistle (1993), (1995)), the balls were moved inwards from the corners to minimise the

stresses at the plate edges, permitting glass sheet to be tested. The load is applied through a neoprene O-ring loaded by a square steel plate with a centralised 4 mm ball to ensure uniformity of loading. With transparent materials, the corners of the test-piece and the square loading plate can be aligned with the vee-grooves to achieve coaxiality. With non-transparent materials, an alternative arrangement needs to be used to ensure the correct positioning of the loading ring.

4. Test-piece preparation

4.1 Dimensions

Test-piece dimensions need to be selected relative to the test-jig design and the availability of materials. As pointed out in Annex B, in order to use the simple linear analysis, the deflection at fracture should be small, typically less than 0.5 of the thickness. This is generally achieved by ensuring that the diameter to thickness ratio is typically less than about 50:1. To avoid wedging effects and the need for corrections, the diameter to thickness ratio should be greater than about 10:1. If the test-jig has a given support ring (or support point circle) diameter, the diameter of the test-piece needs to be larger than this by an amount which is sufficient to avoid risks of local support stresses causing edge shearing. No analysis of this question exists, and in the circumstances it is considered that a similar rule of thumb to that for bar test-pieces could be used, *i.e.* the overhang should be typically not less than the disc thickness.

Much larger overhangs can of course be used; even square plates can be tested with little error (see 2.5), although as the size of the overhang increases, the maximum tangential stress also increases. For materials like glass, this can lead to a risk of edge initiated failures, especially if the edges are machined, but the faces not. In such cases, overhangs need to be either small ($(R - a)/t \sim 1$) or large ($(R - a)/t > 5$), not an intermediate size.

4.2 Edge finish

One of the claimed advantages of biaxial flexure testing compared with bar flexure testing is that the condition of the edges of the test-piece are relatively unimportant as fracture origins, since the stresses are generally low in the overhang region. In contrast, care must be taken with bar testing concerning the condition of edge chamfers, from which failures often occur. Nevertheless, some precautions need to be taken with biaxial test-pieces to ensure that damage is minimal especially for brittle materials like glass. If the test-pieces are derived from pressed discs formed in circular dies, and are round to within about 2% of their diameter, no significant edge finishing is required. However, if discs are prepared by trepanning from flat sheet, the edges may be rather ragged, giving an uncertainty to the measurement of diameter. It may be necessary to perform cylindrical grinding to true them up. On the other hand, since the potential errors in

using square discs and taking the average of the side and diagonal lengths as their effective diameters have been shown to be small, these offer a possibly more convenient geometry provided that the test jig is designed to accommodate them and to align them symmetrically on the support points.

4.3 Surface finish

The surface finish for the test-pieces will depend on the purpose of undertaking the test. No finishing at all is required if the test is intended to search for as-manufactured strength limiting defects. On the other hand, if the test material is available only in bulk, or as discs which are too thick or insufficiently flat for testing, machining will be required, and attention will need to be paid to the quality of the surface.

For uniaxial bar flexure, guidelines are laid down in standards such as CEN EN 843-1, ASTM C1161 and JIS R1601 that permit either a particular sequence of grinding operations, or an application-matched sequence, or a given level of roughness. In particular, it is recommended that the machining direction is parallel to the length of the test-piece. An issue that arises is that unidirectional machining produces anisotropic strength properties, because the damage is anisotropic. Bar test-pieces with the machining direction perpendicular to their length are often weaker than with the machining direction parallel to their length. Comparing uniaxial bar with biaxial disc test results is thus prone to misinterpretation if insufficient allowance is made for directional machining effects. This is particularly important if the test data are to be used for design purposes¹. It is therefore recommended that special care is taken with the specification surface preparation. Isotropic biaxial strengths are more likely to be produced using vertical spindle grinding machines with cup grinding wheels, or by lapping on flat laps, than by using conventional peripheral wheel grinding. Having said this, the general procedures for surface finishing suggested in the uniaxial test standards should be followed where possible.

4.4 Dimensional tolerances

As with bar flexural testing, the critical dimension for accurate calculations is the test-piece thickness. Ideally the thickness should be uniform to within 1%, or better than 0.01 mm per millimetre thickness to ensure that stress errors are minimised. Diameter tolerances can be more relaxed, but discs ideally should be round to 1% of their diameter.

¹ Many of the citations in the scientific literature dealing with the study of biaxial and uniaxial failure from machined test-pieces ignore this point, which can probably explain inconsistencies in results.

An issue which is acknowledged in the literature, but not widely discussed, is that of flatness. For loading systems which are non-compliant, the closeness of conformance of the test-piece to the lines of load contact without distortion determines the degree of match between the true stresses within the test-piece and the analytical values. Strain gauge analyses (*e.g.* Kao *et al.* (1971), Bowles (1973)) have shown that experimental stresses in large plates can be up to 10% different from the analytical expectations, due in part to experimental difficulties and in part to lack of perfect flatness. The use of compliant layers, or compliant or conforming rings may still not completely eliminate the effects of out-of-flatness. Clearly, a balance has to be struck between accuracy achievable and meaningfulness of the test result if special care has to be taken concerning flatness.

Test-piece flatness is an important parameter. It is recommended that for non-compliant contacts, the surface should be flat to better than 0.005 mm over the support circle. For surfaces which are less flat, use compliant layers or conforming supports, but expect experimental errors of up to 10%.

4.5 Number of test-pieces

The same practice as for bar flexural testing should be adopted, *i.e.* 10 test-pieces for determining a mean strength, and at least 30 for characterising the scatter in strengths, *e.g.* through a Weibull analysis.

5. Test procedure

5.1 Measuring test-piece and test-jig dimensions

The test-piece thickness and diameter should be measured at several positions using a calibrated micrometer or vernier callipers, and the averages computed.

The important dimensions on the test jig are the support and loading contact diameters. A travelling microscope is possibly the simplest approach, but first it may be necessary to mark the contact line of a toroidal ring or the contact points of balls by placing them in contact with a dye-coated flat surface (*e.g.* 'engineer's blue' is quite convenient). Linear measurements can then be made between the centres of the markings. Support and loading ring radii should be measured to an accuracy of better than 1% of their dimensions if possible.

5.2 Assembling test-piece and test jig

This will depend to some extent on the design of the test jig, but there are two key points:

- To retain the fragments in position after fracture, place a layer of adhesive tape over the compression side of the test-piece. This is particularly useful for very brittle or for high-strength materials which may fragment into ten or more major pieces plus fine fragments. It simplifies removal of the fractured test-piece from the test jig, and aids subsequent identification of fracture origins. **Do not place the tape on the tensile side - it could contaminate the fracture origin and impede later fractography.**
- The test-piece needs to be correctly aligned on the support system. Some consideration needs to be given to how this is to be done in the simplest possible manner. For disc test-pieces, visual location can be achieved by scribing on the jig base a circle of slightly larger diameter than the test-piece and concentric with the support ring (outside the support position). The test-piece can then be centralised quite accurately by eye relative to this ring. Another possibility is to have a shallow hollow cone aligned coaxially with the loading and support systems which is lowered over the test-piece, pushing it gently to the central position. For square test-pieces, alignment of the corners with two orthogonal scribe lines crossing on the axis of the support and loading system can be effective.

Having positioned the test-piece on the support system, the loading system needs to be correctly positioned, with appropriate load spreaders if required. The jig can then be placed between the compression platens of a conventional mechanical testing machine.

5.3 Conducting the test

Prior experience will permit the selection of an appropriate rate of machine displacement or force application for the test-piece dimensions, loading geometry and compliance of load spreaders. Using displacement rate control will tend to give rather non-linear rates of force development, especially at low force levels, and some authors recommend load control to achieve constant loading rate if the available machine can be controlled in this way. The fracture stresses are then obtained under identical conditions, rather than over a spread of loading rates. Ideally, fracture should occur in 10 s to 20 s. **Care should be taken using load control in compression. Stops must be correctly positioned to prevent overloading jig parts on test-piece failure.**

The peak force is determined either graphically from a force–displacement trace, or from an electronic peak indicator.

5.4 Calculating strength

Normally the simple analytical equations for the peak stress applied to the test-piece are used to calculate the nominal strength of each test-piece. Even if the test-piece breaks outside the region for which the particular equation is valid, the result is still normally calculated in this way. Only if the stress at the point of fracture is required is it necessary to use a more exact method.

5.5 Undertaking fractography

Fractography of biaxial test-pieces is usually rather more difficult than examining bar flexure test-pieces, primarily because there is much more fracture surface to examine. Some useful pointers can normally be obtained from the pattern of radiating and branching cracks, which has received some study by a number of authors (*e.g.* Shetty *et al.* (1983)). Some examples of crack patterns are shown in Figure 7. The number of fragments usually increases with increasing load and reducing toughness. The primary fracture origin is usually near the centre of convergence of these cracks, and lies on the most obvious continuous uninterrupted crack line. Other cracks initiate from this primary crack, and are not continuous across the test-piece.

Once the primary crack has been tentatively identified, it can be inspected by folding the attached adhesive tape along its line to expose both faces. Features seen on this fracture surface will help to identify the position of the origin, unless this is lost by fragmentation. The usual sequence of fractographic investigation can then proceed towards identifying the nature of the origin.

In some cases, the origin will have a preferential orientation, which may leave a small inflection in the trace of the crack at the surface of the test-piece. This is particularly the case if unidirectional machining has been used, producing strength-limiting cracks aligned with the machining direction.

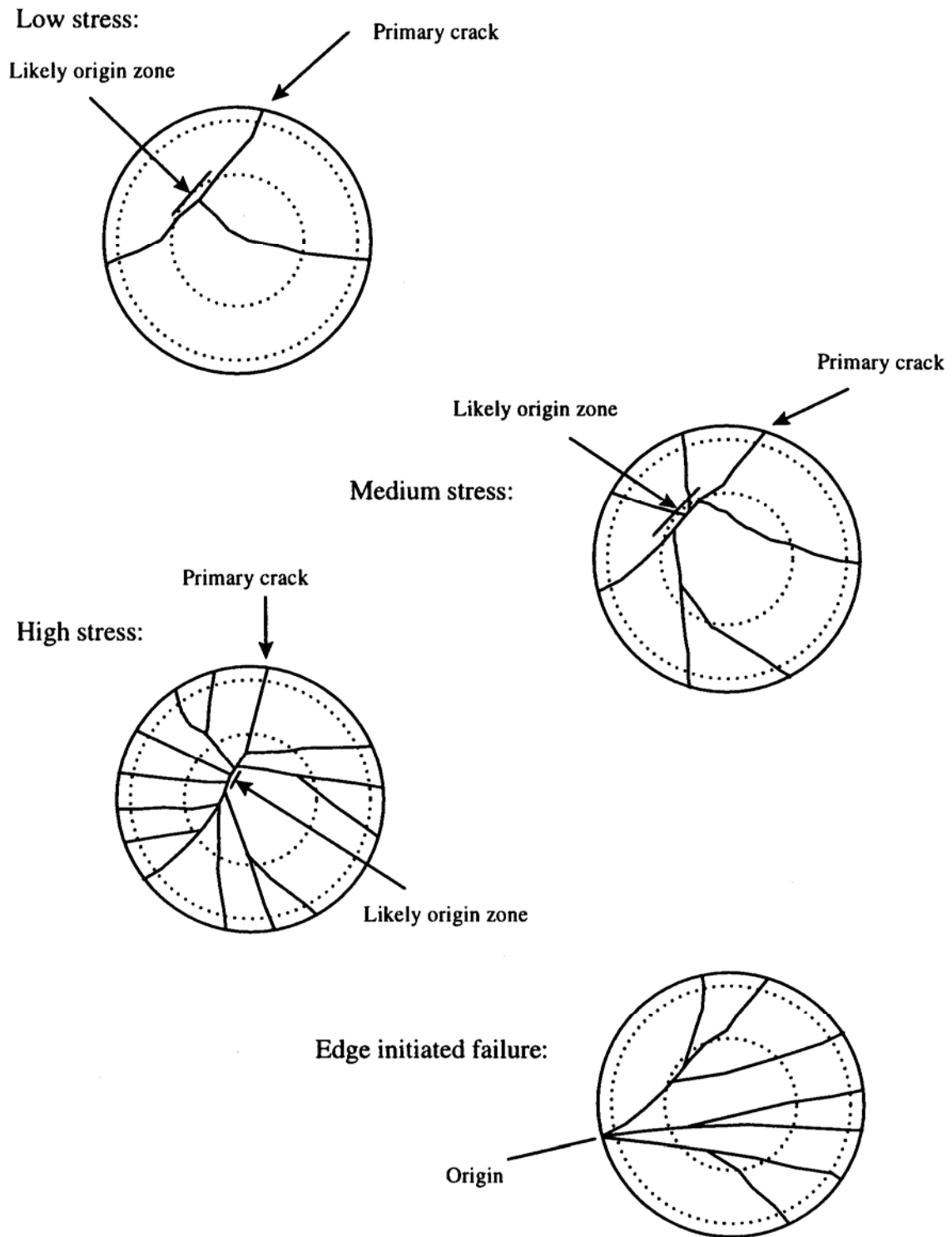


Figure 7 - Typical fracture patterns in disc test-pieces.

6 Comparison of biaxial and uniaxial strengths

There are numerous references in the literature to investigations of this relationship, notably in regard to Weibull size scaling theories and multiaxial fracture criteria. A full discussion of this information is not within the purpose of this guide. However, the general finding is that biaxial strengths determined from disc test-pieces are often lower than would be predicted from uniaxial tests using typical multiaxial failure criteria and Weibull stressed volume or area extrapolation techniques. The reasoning behind this is not clear, but may be associated with the preparation of test-pieces. Some possible factors are:

- Discs are frequently made by different powder shaping techniques to those for bars, and thus may conceivably have different volume flaw distributions unless precautions are taken to ensure the same billet material is used for both types of test.
- The sampling of volume defects involved in selecting small bar test-pieces may not be the same as in larger discs, resulting in different volume flaw distributions revealed by the respective tests.
- The surface preparation techniques may be different. Face machining of disc test-pieces typically requires either a peripheral diamond wheel giving a unidirectional finish, or a cup or face wheel, or lapping, giving multidirectional grinding. Machining of bars is generally performed with a peripheral grinding wheel parallel to the test-piece length, the procedure recommended in standards. It is known that bar strengths depend on the direction of grinding, so the strength of discs prepared in the same way as bars will be anisotropic, and will therefore reflect the weakest direction rather than that normally encountered in bars. Efforts need to be made to ensure that the comparison is made on the basis of proper selection and control of surface finishing procedures.
- The strength of discs is normally independent of the quality of edge finish, but that of bars may depend on how chamfers are prepared. More generally, it is important to ensure that the flaw types initiating failure are similar for the two geometries.

The following points are recommended:

- **Ensure that the material for the tests comes from the same billet material – directly prepared test-pieces may have different flaw distributions.**
- **Select grinding procedures which are equivalent for the two types of test and, if directional, which reflect the weakest direction in testing.**
- **Use fractography to ensure that similar flaw types act as fracture origins in all cases.**

7 Use of biaxial testing for subcritical crack growth and fracture toughness tests

A number of examples in the literature demonstrate that, generally speaking, delayed failure and certain types of fracture toughness determinations can be performed using disc tests. The biaxial tensile stress field seems to have little influence on opening mode crack development and propagation, although the same might not be true with other forms of biaxial stress.

Examples of materials in which subcritical crack growth has been evaluated through tests covering a wide range of stressing rates include cordierite glass-ceramics (Baskaran *et al.* (1985)), various glasses and glass-ceramics (Ikeda and Tamiaki (1993)), and alumina (Chao and Shetty (1994)). A conclusion appears to be that the equibiaxial stress state found in disc flexure testing enhances subcritical crack growth compared with uniaxial testing by making it easier for a propagating crack to deviate around obstacles, even if the fatigue parameter n has a similar value to that obtained in uniaxial testing.

Cyclic fatigue tests have been performed using a modified ring on ring system by Hulm *et al.* (1996) to determine characteristics of aluminas and zirconias for orthopaedic implant purposes.

Fracture toughness testing of alumina using the indentation fracture technique in which an indentation is made in the tensile central zone of a ring/ring test-piece is reported by Fernandes *et al.* (1993). Chen and Ardell (1996) report the use of very small test-pieces of a variety of materials, only 3 mm diameter and 250 μm to 400 μm thick, with some limitations on reproducibility.

8 Tests at raised temperatures

One of the immediate problems with undertaking biaxial tests at raised temperature is that the use of any soft interlayer materials, such as rubber or paper, for the purpose of improving uniformity of contact or reducing friction is clearly no longer feasible. Thus additional efforts must be made to ensure that test-piece surfaces and loading contacts are directly conforming to achieve uniformity of loading. Friction effects remain a problem, and further considerations of jig design must be made if this problem is to be solved.

There is actually very little research on high-temperature biaxial testing reported in the literature. Giovan and Sines (1981) tested an alumina ceramic using a test jig made with Inconel 718 loading and support rings, the loading ring being attached to a rod guided by two parallel compliant flexure plates of the same material. This arrangement was said to ensure accurate axial movement and positioning of the loading ring relative to the support ring. The temperature limit for the apparatus was 982 °C. Quinn and Wirth (1988) report biaxial static fatigue tests on

a hot-pressed silicon nitride using the ring-on-ring geometry. The rings were made from tubes of recrystallised silicon carbide on which half-toroids were machined to give nominal support and loading ring diameters of 40 mm and 10 mm respectively. Tests were conducted at 1200 °C and 1300 °C for periods of up to 100 h with no problems of loading contact contamination. The principal findings were that in addition to the room temperature, short-term strength of the test material being significantly less than uniaxial flexural strength, the stress rupture lifetimes were also significantly shorter by one to two orders of magnitude, but with a similar trend with stress applied. The fracture behaviour was variable, and the authors attributed this to complex redistribution of stress as cracks developed, especially at low stress. They concluded that the test method could be interpreted properly only for small plastic deflections and short subcritically-grown crack sizes.

9 Conclusions

Disc testing has not had the same detailed technical attention that bar testing has received over the last decade, and therefore has no developed pedigree. The large number of geometries that are available provide the user with a range of options and uncertainties which only further research can hope to reduce.

If the purpose of the testing is for quality control, the details of test geometry are much less important than for design data collection. For the latter, it is advised that caution be exercised in three key areas:

- Select test-piece and test jig geometries which do not invite significant errors due to:
 - large deformations at fracture
 - lack of compensation for friction
 - poorly-defined geometry and inaccuracy of dimensional measurement
- Select surface finishing procedures relevant to the end application, but ensure that if comparisons with other shapes of test-piece or stressing modes are to be made, the directionality of the procedures is understood and the results are correctly interpreted.
- If test-pieces are not geometrically flat, adopt procedures which either rely on three-ball support, or which incorporate compliant interlayers or compliant contact surfaces.

10. Bibliography

- Adler, W.F.; Mihora, D.J. (1992), Biaxial flexure testing: analysis and experimental results, *Fracture Mechanics of Ceramics* **10**, edited by Bradt, R.C.; Hasselman, D.P.H.; Munz, D.; Sakai, M.; Shevchenko, V.Ya, Plenum Press, New York, pp. 227–45.
- Baskaran, S.; Bhaduri, S.B.; Hasselman, D.P.H. (1985), Effect of crystallites on subcritical crack growth and strain rate sensitivity of strength of cordierite glass-ceramics, *J. Amer. Ceram. Soc.*, **68**(3), 112–9.
- Bowles, R. (1973), Strength tests for flat glass samples, *Technical Note No. 170*, British Glass Industry Research Association, Sheffield, UK.
- Chao, L.-Y.; Shetty, D.K. (1994), Time-dependent strength degradation and reliability of an alumina ceramic subjected to biaxial flexure, in *Life Prediction Methodologies and Data for Ceramic Materials*, Cocoa Beach, Florida, USA, Jan. 1993, ASTM STP 1201, edited by Brinkman, C.R.; Duffy, S.F., pp. 228–49.
- Chen, F.C.; Ardell, A.J. (1996), Fracture toughness of brittle materials from small disk-shaped specimens, *Innovations in Mater. Res.*, **1**(1), 47–64.
- Entwhistle, K.M. (1991). The fracture of concentrically loaded square ceramic plates, *J. Mater. Sci.*, **26**, 1078–86.
- Entwhistle, K.M. (1993). The fracture stress of float glass, *J. Mater. Sci.*, **28**, 2007–12.
- Entwhistle, K.M. (1995). A fracture test using concentrically loaded square plates, *J. Mater. Sci.* **30**, 3773–81.
- Evans, A.G.; Davidge, R.W. (1971), A bi-axial stress method for the determination of the strength of sections cut from glass containers and the size of critical Griffith flaws, *Glass Technol.* **12**(6), 148–54.
- Fernandes, J.J.; Guerra Rosa, L., Morrell, R. (1993), Fracture toughness using a biaxial indentation strength method, *Euroceramics III*, **3**, 907–911.
- Fessler, H.; Fricker, D.C. (1984), A theoretical analysis of the ring-on-ring loading disk test, *J. Amer. Ceram. Soc.*, **67**(9), 582–8, Correction: *ibid*, 1988, **71**(10), 904.
- Furguiele, F.M.; Lamberti, A.; Poggialini, A. (1995), Monitoring of biaxial tests of ceramic materials by digital speckle interferometry, *Experimental Techniques*, **19**(5), 15–19.

- Furguiele, F.M.; Muzzupappa, M., Pagnotta, L. (1997), A full-field procedure for evaluating the elastic properties of advanced ceramics, *Experimental Mechanics*, **37**(3) 285–91.
- Giovan, M.N.; Sines, G. (1981), Strength of a ceramic at high temperatures under biaxial and uniaxial tension, *J. Amer. Ceram. Soc.*, **64**(2), 68–73.
- Godfrey, D.J. (1985), Fabrication, formulation, mechanical properties and oxidation of sintered silicon nitride using disc specimens, *Mater. Sci. Technol.*, **1**(7), 510–5.
- Godfrey, D.J.; John, S. (1986), Disc flexure tests for evaluation of ceramic strength, *Proc. Second Intl. Symp. Ceramic Materials and Components for Engines*, Lübeck-Travemünde, Germany, edited by Bunk, W., Hausner, H., Verlag Deutsche Keramische Ges. 1986, pp 657–65.
- Hulm, B. J.; Parker, J.D.; Evans, W.J. (1996), The use of ceramic materials for femoral head replacement, *Proc. Conf. Frontiers for Engineering Materials, IMF 11, September 1995*, published as *Key Engineering Materials*, **118–9**, 321–8.
- Ikeda, K.; Tamiaki, M. (1993), Study for fatigue behaviour of glass ceramics under multiaxial stress states, *Mem. Fac. Eng. Miyazaki Univ.* (22), 51–81.
- Kirstein, A.F.; Woolley, R.M. (1967), Symmetrical bending of thin circular elastic plates on equally spaced supports, *J. Res. NBS*, **71C**, 1–10.
- Manley, M.E.; Ertürk, T.; Vaucamps, C.; Gailus, D. (1994), Four-point and biaxial flexure strength of PZT ceramics: a probabilistic approach, *Cer. Eng. Sci. Proc.*, **15**(4) 885–94.
- Marshall, D.B. (1980), An improved biaxial flexure test for ceramics, *Bull. Amer. Ceram. Soc.*, **59**(5), 551–3.
- Matthewson, M.J.; Field, J.E. (1980), An improved strength measurement technique for brittle materials, *J. Phys. E (Sci. Instr.)*, **13**(3), 355–9.
- Morrell, R. (1988), unpublished results of a UK round robin.
- Morrell, R.; McCormick, N.J.; Bevan, J.; Lodeiro, M.; Margetson, J. (1998), Biaxial disc flexure, *IoM Ceramics Convention, April 1998, Royal Agricultural College*, publ. in *Brit Cer. Proc.*, 1999, **59**, 31-44 and *Brit Ceram. Trans.* 1999, **98**(5), 234-40.

- Newton, J.M.; Gaspe, A.G.B.; Hand, R.J.; Messer, P.F. (1995), Apparatus for disc biaxial flexure and ring burst testing of large ceramic specimens, *Brit. Ceram. Trans.*, **94**(6), 246–9.
- Quinn, G.D.; Wirth, G. (1988), Biaxial static fatigue of silicon nitride, *Mater. Sci. Eng. A*, **A109**, 147–152.
- Ritter, J.E., Jr.; Jakus, K.; Batakis, A.; Bandyopadhyay, N. (1980), Appraisal of biaxial strength testing, *J. Non-Cryst. Solids*, **28/9**, 418–29.
- Roark, R.J.; Young, W.C. (1975), *Formulas for stress and strain*, McGraw Hill Book Co., New York, USA, 5th edition.
- Shetty, D.K.; Rosenfield, A.R.; McGuire, P.; Bansal, G.K.; Duckworth, W.H. (1980), Biaxial flexure tests for ceramics, *Bull. Amer. Ceram. Soc.*, **59**(12), 1193–7.
- Shetty, D.K.; Rosenfield, A.R.; Duckworth, W.H. (1983), Crack branching in ceramic disks subjected to biaxial flexure, *J. Amer. Ceram. Soc.*, **66**(1), C-10–C-12.
- Soltész, U.; Richter, H.; Kienzler, R. (1987), The concentric ring test and its application for determining the surface strength of ceramics, *Proc. Conf. Ceramics in Clinical Applications*, 26-8 June 1986, Milan, published as *High-Tech Ceramics*, edited by Vincenzini, P., Elsevier Science Publishers B.V., Amsterdam, pp. 149–58.
- Timoshenko, S.; Woinowsky-Krieger, P (1959), *Theory of plates and shells*, McGraw Hill Book Co., New York, 2nd edition, p72.
- Vitman, F.F.; Pukh, V.P. (1963), A method for determining the strength of sheet glass, *Aavodskaya Laboratoriya (Industrial Laboratory)*, **29**, 863–67 (in Russian).
- Wachtman, J.B., Jr., Capps, W.; Mandel, J. (1972), Biaxial flexure tests of ceramic substrates, *J. Materials (JMLSA)*, **7**, 188–94.
- Wilshaw, T. (1968), Measurement of tensile strength of ceramics, *J. Amer. Ceram. Soc.*, **51**(2), 111.

Annex A – Determination of elastic properties using the impact excitation method on disc test-pieces

A.1 Introduction

All the equations for calculating nominal biaxial flexural strength require the insertion of a value for Poisson's ratio, ν . Traditionally, Poisson's ratio has been obtained from separate determinations of Young's modulus E and shear modulus G , for example by strain gauge techniques, resonance techniques, or ultrasonic longitudinal and shear wave velocity determinations. However, one of the simplest methods of determining an appropriate value for biaxial strength calculations is to use the same test-piece (if large enough) and determine ν directly from its vibration frequencies. The first two modes of vibration of a disc test-piece are the 'saddle mode' and the 'diaphragm' mode. If a disc test-piece is resonated or struck appropriately, and the two frequencies determined, then assuming that the elastic properties are homogeneous and isotropic, Poisson's ratio, Young's modulus and hence shear modulus can all be determined from the same test-piece. This Annex deals with the details of the method, which is currently (1998) being balloted as an extension to the impact excitation method standard ASTM C1259 for advanced technical ceramics.

A.2 Disc vibration modes and test principle

The analysis of natural disc vibration originates from Colwell and Hardy (1937), and was developed as a means for determining Poisson's ratio by Martincek (1965). This work was subsequently employed by Glandus (1981) in his thesis on strength and thermal shock resistance of ceramic materials. A disc resonated or struck at its centre vibrates axisymmetrically with antinodes at the centre and periphery, with a ring node positioned at 0.681 of the disc radius. For the purposes of this Annex, this is the 'diaphragm' or second mode, which is of higher frequency than the first or 'saddle' mode in which orthogonal diameters flex in opposite directions (the antilexural mode), leaving two orthogonal nodal diameters at 45° to the antinodal diameters. The difference between the modes can be readily heard on a large disc of material.

A.3 Test method

To determine the elastic properties of the disc, the main steps are as follows:

- determine the mass (m) and dimensions (thickness, t , and radius, R) of the test-piece;

Impact excitation of discs - modes

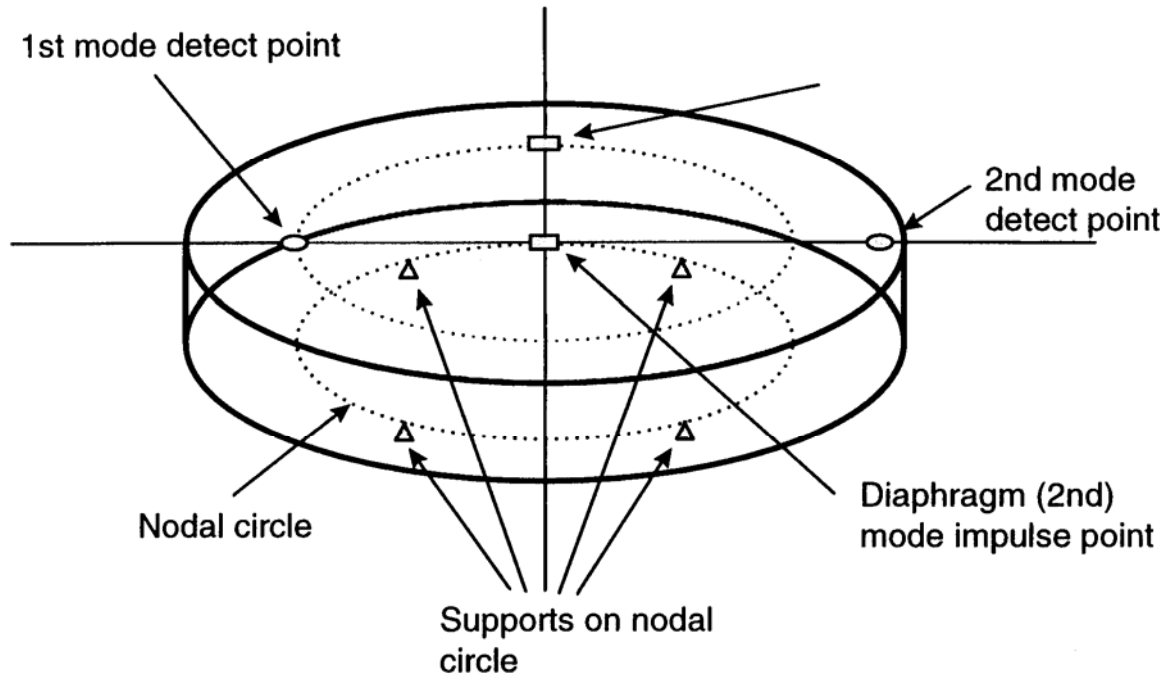


Figure A.1 - Impact excitation of discs - impact and detection positions.

- measure the frequencies of the two modes and calculate their ratio (f_2/f_1);
- estimate Poisson's ratio using a look-up table (Table A1) which requires also the ratio of thickness to radius (t/R);
- calculate two Young's modulus values from the formula:

$$E_{1,2} = \frac{37.6991 f_{1,2}^2 d^2 m (1 - \nu^2)}{K_{1,2}^2 t^3} \quad (\text{A.1})$$

where subscripts 1, 2 refer to the first and second modes respectively, and $K_{1,2}$ are geometrical constants obtained from further look-up tables (Tables A2) for given values of ν and t/R .

- calculate the mean of the two values of Young's modulus;

- calculate shear modulus from Young's modulus and Poisson's ratio:

$$G = \frac{E}{2(1 + \nu)} \quad (\text{A.2})$$

It will be noted that unlike methods for determining elastic properties from bar test-pieces, the first parameter to be calculated is Poisson's ratio which can be determined much more accurately than from separate measurements of E and G and the reverse use of Equation A2. This of course assumes that the look-up table derived from Glandus (1981) is as accurate as the three-figure precision with which it is given.

It can also be noted that for small t/R ratios, less than 0.1, the value obtained for ν is essentially independent of t/R . This clearly simplifies calculation, because interpolation of the table can be made using the equation:

$$\nu = -0.5609 \left(\frac{f_2}{f_1} \right)^2 + 2.5717 \left(\frac{f_2}{f_1} \right) - 2.4209 \text{ for } t/r = 0.05 \quad (\text{A.3})$$

$$\nu = -0.475 \left(\frac{f_2}{f_1} \right)^2 + 2.959 \left(\frac{f_2}{f_1} \right) - 2.213 \text{ for } t/r = 0.2$$

with an accuracy of ν about ± 0.001 , a level which would be very difficult to achieve by any other technique. For test-pieces made from pressed discs the t/R ratio is typically between 0.1 and 0.4, and the tables must be interpolated by inspection. Tables A2 contain data for an expanded region to assist interpolation. There are currently no satisfactory single algebraic formulations to represent the tables without loss of accuracy.

A.4 Experimental technique

The test disc can be either driven by a variable frequency driver/detector system as for the resonance method, or it can be struck and the principal frequencies determined using a microphone or piezo-detector².

It is important that the disc is parallel-faced and round to good precision (± 0.02 mm or $\pm 0.01\%$, whichever is the larger, is a convenient target). Failure to achieve such precision results in two

² In trials at NPL, the impact excitation method has been used, with the frequencies detected either by a carefully positioned piezo-detector or by a microphone. The frequencies can be determined by a proprietary instrument such as the 'Grindosonic' (Lemmens Elektronika BV, Leuven, Belgium), or more reliably using a dynamic signal analyser to give a Fourier transform frequency spectrum. The latter often allows both frequencies to be determined simultaneously, and is especially useful at higher test-piece temperatures.

closely spaced frequencies rather than a single frequency for each mode, increasing the uncertainty rather more than simply from the errors of measurement of disc dimensions would lead one to expect. A similar effect will also arise if the disc does not have homogeneous properties, or if the edge is badly chipped or cracked.

For a large disc, the support material is most conveniently rubber, such as four small arcs cut from a rubber O-ring, which should be positioned at four equally spaced points around the nodal circle. To do this, draw a circle of slightly larger diameter than the test disc on a piece of paper, and another concentric circle at 0.681 of the disc diameter (the nodal circle). Place the four supports on this latter circle, and position the disc on them and to be visually concentric with the larger circle. For a small disc, this mode of positioning can be tricky, but satisfactory results can be obtained if the disc is simply supported on a bed of ceramic fibre or similar medium which does not couple mechanically to the disc.

For the first, ‘saddle’ mode, strike or drive the disc on the nodal circle mid-way between the support positions, and if using a piezo-detector, detect the vibrations on the nodal circle mid-way between another pair of support points (Figure A1). At this point, the second ‘diaphragm’ mode vibrations will be at a minimum. For the second mode, drive or strike the disc at the centre (which is a node for the first mode) and detect the vibration at the disc periphery along a radius intersecting a support point (a nodal line for the first mode). Either scan the driving frequency, or repeat the striking until the repeatable results are obtained.

A.5 Limitations

The test has been found to work well on most types of ceramic disc provided that the aspect ratio of the disc (t/R) and the disc diameter ($d = 2R$) are suitable, such that the frequencies are conveniently detectable. For large discs, say 100 mm diameter, there is usually no problem with detection, but the two frequencies for ceramic discs smaller than about 40 mm are in the 10s of kHz. The microphone system and amplifier need to have a range far wider than normal audio. The method becomes essentially unusable when the disc is less than 20 mm diameter and the higher of the two frequencies is above 100 kHz because of the difficulties of accurately striking or driving the disc.

An example of test results on small discs compared with bar test-pieces using the impact excitation method is given in Table A3. The test materials were chosen to be homogeneous and well characterised. There is good equivalence of Young’s modulus between the two types of test-piece, and Poisson’s ratio values are typical of ‘book’ values for these materials. Some tests on larger test-pieces and to higher temperatures are reported by Morrell *et al.* (1998).

A.6 Bibliography

Colwell, R.C.; Hardy, H.C. (1937), The frequencies and nodal systems of circular plates, *Phil. Mag.*, **S7**, **24**(165) 1041–55.

Glandus, J.C. (1981), Rupture fragile et résistance aux chocs thermiques de céramiques a usages mécaniques, thesis, University of Limoges, France.

Martinec, G. (1965), The determination of Poisson's ratio and dynamic modulus of elasticity from the frequencies of natural vibration in thick circular plates, *J. Sound Vibration*, **2**(2), 116–27.

Morrell, R.; McCormick, N.J.; Bevan, J.; Lodeiro, M.; Margetson, J. (1998), Biaxial disc flexure – modulus and strength testing, *IoM Ceramics Convention, April 1998, Royal Agricultural College*, publ. in *Brit Cer. Proc.*, 1999, **59**, 31-44 and *Brit Ceram. Trans.* 1999, **98**(5), 234-40.

Table A.1 – Look-up table for Poisson's ratio (after Glandus (1981))

	Poisson's ratio for frequency ratios, f_2/f_1 , of											
t/R	1.350	1.375	1.400	1.425	1.450	1.475	1.500	1.525	1.550	1.575	1.600	1.625
0.00	0.015	0.043	0.070	0.094	0.118	0.141	0.163	0.184	0.205	0.226	0.247	0.265
0.05	0.018	0.044	0.070	0.094	0.118	0.141	0.164	0.185	0.206	0.226	0.247	0.265
0.10	0.020	0.045	0.070	0.094	0.118	0.141	0.164	0.185	0.206	0.227	0.247	0.265
0.15	0.023	0.049	0.075	0.100	0.124	0.148	0.171	0.192	0.212	0.233	0.254	0.271
0.20	0.025	0.053	0.080	0.105	0.130	0.154	0.178	0.198	0.218	0.239	0.260	0.278
0.25	0.033	0.060	0.088	0.114	0.139	0.162	0.186	0.206	0.227	0.247	0.268	0.286
0.30	0.040	0.068	0.096	0.122	0.148	0.171	0.193	0.214	0.235	0.255	0.275	0.294
0.35	0.051	0.078	0.105	0.130	0.155	0.179	0.203	0.224	0.245	0.264	0.284	0.302
0.40	0.062	0.088	0.113	0.138	0.162	0.187	0.212	0.234	0.255	0.274	0.292	0.310
0.45	0.070	0.096	0.123	0.148	0.173	0.197	0.221	0.242	0.263	0.281	0.300	0.318
0.50	0.078	0.105	0.132	0.158	0.183	0.206	0.229	0.250	0.270	0.289	0.307	0.327
	Poisson's ratio for frequency ratios, f_2/f_1 , of											
t/R	1.650	1.675	1.700	1.725	1.750	1.775	1.800	1.825	1.850	1.875	1.900	
0.00	0.282	0.297	0.312	0.329	0.346	0.362	0.378	0.394	0.409	0.424	0.438	
0.05	0.283	0.298	0.314	0.331	0.347	0.363	0.378	0.394	0.409	0.424	0.438	
0.10	0.283	0.300	0.316	0.332	0.348	0.363	0.378	0.394	0.409	0.424	0.438	
0.15	0.289	0.306	0.322	0.338	0.354	0.368	0.383	0.398	0.413	0.427	0.442	
0.20	0.295	0.312	0.328	0.344	0.359	0.374	0.388	0.403	0.417	0.431	0.445	
0.25	0.304	0.320	0.336	0.351	0.366	0.380	0.395	0.409	0.423	0.437	0.451	
0.30	0.312	0.328	0.344	0.358	0.372	0.387	0.402	0.415	0.428	0.442	0.456	
0.35	0.320	0.336	0.352	0.367	0.382	0.398	0.414	0.428	0.442	0.456	0.471	
0.40	0.328	0.344	0.360	0.376	0.392	0.409	0.425	0.440	0.455	0.470	0.485	
0.45	0.337	0.354	0.370	0.387	0.403	0.420	0.437	0.452	0.468	0.485	0.503	

Measurement Good Practice Guide No. 12

0.50	0.346	0.363	0.380	0.397	0.414	0.431	0.448	0.464	0.480	0.500	0.520
------	-------	-------	-------	-------	-------	-------	-------	-------	-------	-------	-------

Table A.2 – Look-up tables for K_1 and K_2 (after Glandus (1981))

v	K_1 values for first mode calculation for values of t/R										
	0.00	0.05	0.10	0.15	0.20	0.25	0.30	0.35	0.40	0.45	0.50
0.00	6.170	6.144	6.090	6.012	5.914	5.800	5.674	5.540	5.399	5.255	5.110
0.05	6.076	6.026	5.968	5.899	5.816	5.717	5.603	5.473	5.331	5.178	5.019
0.10	5.962	5.905	5.847	5.782	5.705	5.613	5.504	5.377	5.234	5.079	4.915
0.15	5.830	5.776	5.720	5.657	5.581	5.490	5.382	5.256	5.115	4.962	4.800
0.20	5.681	5.639	5.587	5.524	5.446	5.351	5.240	5.114	4.975	4.826	4.673
0.25	5.517	5.441	5.445	5.380	5.297	5.197	5.083	4.957	4.822	4.681	4.537
0.30	5.340	5.331	5.290	5.223	5.135	5.030	4.913	4.787	4.656	4.523	4.390
0.35	5.192	5.156	5.120	5.052	4.961	4.853	4.734	4.610	4.483	4.358	4.234
0.40	4.973	4.964	4.931	4.865	4.775	4.668	4.551	4.429	4.306	4.186	4.070
0.45	4.781	4.756	4.723	4.661	4.576	4.476	4.365	4.249	4.131	4.013	3.899
0.50	4.540	4.525	4.490	4.436	4.365	4.280	4.182	4.075	3.960	3.841	3.720
v	K_1 values for first mode calculation (emboldened region expanded) for values of t/R										
	0.10	0.11	0.12	0.13	0.14	0.15	0.16	0.17	0.18	0.19	0.20
0.14	5.746	5.739	5.722	5.710	5.696	5.683	5.670	5.654	5.642	5.629	5.608
0.16	5.694	5.687	5.670	5.664	5.645	5.632	5.619	5.602	5.590	5.576	5.556
0.18	5.641	5.634	5.617	5.606	5.592	5.579	5.566	5.549	5.537	5.523	5.502
0.20	5.587	5.576	5.563	5.551	5.538	5.524	5.510	5.495	5.479	5.463	5.446
0.22	5.531	5.524	5.507	5.495	5.481	5.468	5.455	5.439	5.427	5.411	5.388
0.24	5.474	5.467	5.450	5.438	5.424	5.410	5.396	5.379	5.366	5.351	5.328
0.26	5.415	5.408	5.391	5.379	5.364	5.350	5.336	5.318	5.304	5.289	5.266
0.28	5.354	5.347	5.330	5.317	5.301	5.287	5.273	5.255	5.241	5.225	5.201
0.30	5.290	5.279	5.266	5.253	5.238	5.223	5.207	5.190	5.173	5.154	5.135
0.32	5.224	5.217	5.200	5.187	5.172	5.157	5.142	5.123	5.108	5.091	5.067
0.34	5.156	5.148	5.131	5.118	5.103	5.088	5.073	5.053	5.037	5.020	4.997
v	K_2 values for first mode calculation for values of t/R										
	0.00	0.05	0.10	0.15	0.20	0.25	0.30	0.35	0.40	0.45	0.50
0.00	8.240	8.226	8.151	8.027	7.863	7.670	7.455	7.227	6.991	6.754	6.520
0.05	8.378	8.339	8.252	8.124	7.963	7.777	7.570	7.350	7.120	6.885	6.649
0.10	8.511	8.459	8.364	8.233	8.071	7.885	7.679	7.459	7.228	6.991	6.751
0.15	8.640	8.584	8.485	8.349	8.182	7.990	7.779	7.553	7.316	7.074	6.830
0.20	8.764	8.712	8.611	8.469	8.294	8.092	7.871	7.635	7.390	7.141	6.889
0.25	8.884	8.840	8.738	8.589	8.403	8.189	7.954	7.706	7.450	7.191	6.931
0.30	9.000	8.962	8.860	8.705	8.508	8.280	8.030	7.767	7.497	7.226	6.960
0.35	9.111	9.081	8.977	8.814	8.605	8.363	8.098	7.819	7.535	7.253	6.979
0.40	9.219	9.193	9.085	8.913	8.692	8.436	8.157	7.865	7.569	7.276	6.991
0.45	9.321	9.292	9.178	8.997	8.766	8.499	8.208	7.905	7.598	7.295	7.001
0.50	9.420	9.376	9.252	9.063	8.824	8.550	8.252	7.940	7.625	7.313	7.010
v	K_2 values for first mode calculation (emboldened region expanded) for values of t/R										
	0.10	0.11	0.12	0.13	0.14	0.15	0.16	0.17	0.18	0.19	0.20
0.14	8.460	8.443	8.411	8.385	8.355	8.326	8.297	8.262	8.234	8.202	8.160
0.16	8.510	8.493	8.460	8.433	8.403	8.373	8.343	8.308	8.279	8.248	8.205
0.18	8.560	8.542	8.509	8.482	8.451	8.421	8.391	8.356	8.327	8.294	8.249
0.20	8.611	8.586	8.559	8.530	8.500	8.469	8.437	8.403	8.368	8.331	8.294
0.22	8.662	8.646	8.613	8.582	8.548	8.517	8.487	8.454	8.425	8.390	8.338
0.24	8.712	8.694	8.660	8.630	8.597	8.565	8.534	8.498	8.467	8.432	8.382
0.26	8.762	8.743	8.708	8.678	8.645	8.612	8.580	8.542	8.510	8.474	8.425
0.28	8.811	8.791	8.755	8.726	8.692	8.659	8.625	8.585	8.551	8.515	8.467
0.30	8.860	8.833	8.804	8.772	8.739	8.705	8.668	8.630	8.591	8.550	8.508
0.32	8.907	8.885	8.848	8.818	8.784	8.750	8.716	8.675	8.640	8.601	8.548
0.34	8.954	8.932	8.894	8.863	8.827	8.793	8.758	8.717	8.681	8.641	8.586

Table A.3 – Comparison of disc and bar results for impact excitation modulus testing

Material	Density, Mg m ⁻³	Test-piece dimensions, mm	Discs, impact excitation			Bars, impact excitation, E, GPa	Discs, as for impact excitation, ultrasonic velocity		
			E, GPa	G, GPa	v		E, GPa	G, GPa	v
Translucent alumina	3.963 ± 0.003	23 Ø x 3	392.7 ± 4.1	158.6 ± 1.6	0.238 ± 0.001	396.8 ± 4.5	397.8 ± 0.5	158.7 ± 0.3	0.254 ± 0.002
98% alumina	3.826 ± 0.007	30 Ø x 3	361.6 ± 2.0	145.7 ± 0.7	0.242 ± 0.005	358.8 ± 4.2	355.3 ± 5.6	140.1 ± 3.0	0.257 ± 0.007
Zirconia, partially stabilised	5.412 ± 0.008	30 Ø x 3	184.4 ± 1.4	71.5 ± 1.0	0.289 ± 0.011	180.4 ± 3.0	192.0 ± 1.2	75.12 ± 0.37	0.278 ± 0.002
'Macor' machinable glass-ceramic	2.533 ± 0.004	30 Ø x 3	64.18 ± 0.11	25.32 ± 0.05	0.268 ± 0.001	64.84 ± 1.22	65.76 ± 0.19	26.19 ± 0.09	0.259 ± 0.002
Fused silica	2.200 ± 0.001	30 Ø x 3	72.72 ± 0.09	30.84 ± 0.05	0.180 ± 0.004	72.69 ± 0.67	75.50 ± 0.35	32.29 ± 0.15	0.169 ± 0.004

Annex B – Large deflection analysis for thin discs

B.1 Introduction

The central deflection of a disc test-piece subjected to ring/ring loading has been given by Vitman and Pukh (1963) as³:

$$w_0 = \frac{3F(1-\nu^2)}{2\pi Eht^3} \left[a^2 + \frac{a^2(1-\nu)(a^2-b^2)}{2(1+\nu^2)R^2} - b^2 \left(1 + \ln\left(\frac{a}{b}\right)\right) \right] \quad (\text{B.1})$$

However, it is recognised that this simple analytical solution is valid only for thin discs which do not deflect significantly. If the deflection becomes of the same order as the thickness of the disc, the deflections and the stress distribution are no longer linear with applied force. So-called ‘membrane stresses’ are set up which have the effect of reducing the deflection below that of simple linear theory, and similarly, for the ring-on-ring geometry, of reducing the maximum tensile stress but creating a ring-shaped stress concentration under the loading ring.

B.2 Analysis

There is no simple analytical equation for relating stresses to applied forces, and the problem cannot be solved simply by analytical means. Timoshenko and Goodier (1970) give examples of solutions for central displacements in uniformly pressurised discs with clamped edges, but these are not relevant to the condition of free edge support with overhang used in the testing of ceramics. Kao *et al.* (1971) used a set of non-linear finite difference equations to replace the non-linear differential equations that need to be solved. They showed that for the case of glass sheet, their technique gave results which matched those of Timoshenko and Woinowsky-Krieger (1959) for the clamped edge case with uniform pressure loading. They went on to explore the situation for the free-edge with overhang, ring supported/ring loaded geometry, assuming no friction at the contacts. For the specific case of Poisson’s ratio being 0.21, ring radii ratio $a : b$ being 2, and the disc radius to support ring radius ratio being 1.1, their results have been reworked in Figures B.1 and B.2 to give, in non-dimensional terms, respectively the deflections and the maximum tensile stresses at the centre and under the loading ring. It can be seen that the initially linear deflection behaviour is soon lost when the central displacement exceeds about 0.5 of the disc thickness (i.e. $w_0/t > 0.5$) which is achieved when the non-dimensional force applied is greater than about 2 (i.e. $Fa^2/Et^4 > 2$). At this point, the non-dimensional stress $\sigma a^2/Et^2$ exceeds about 1 where σ is the true stress. A guide to the requirement for undertaking non-linear analysis can be obtained from the following equation:

³ This equation, and the corresponding ones for stress, can be derived in a number of ways, and have recently been independently checked at NPL.

$$\frac{\sigma a^2}{E t^2} \geq 1 \quad \text{or when} \quad t \leq a\sqrt{\varepsilon_f} \quad (\text{B.2})$$

Since in a fracture test, the strain at failure, $\varepsilon_f = \sigma_f/E$, is typically in the range 0.0005 to 0.003, depending on the type of material, non-linear analysis will be required when the support ring radius to thickness ratio, a/t , is greater than about 50 for a weak material or about 20 for a very strong material.

The same authors also computed relationships for the case where the load ring radius to support ring radius is 0.2, rather than 0.5 in the above case. They found that the homogeneity of the central zone stress field is much less problematical. This suggests that a smaller loading ring radius has some distinct advantages compared with the case analysed above.

There is other literature in the public domain which permits analysis of other conditions:

1. Ferriss (1984, 1991) has dealt with the cases of simply supported and clamped edge plates subjected to uniform or centrally applied forces, deriving equations which relate the maximum tensile stress occurring at the plate centre to the deflection via a parabolic relationship, the constants in which are related to Poisson's ratio.
2. The International Energy Agency (IEA) programme task on fuel cell materials has applied finite element analysis to incremental displacements of a thin planar disc subjected to ring supported/ring loaded flexure. This work has not been fully published, but a summary is available in Kübler *et al.* (1995) dealing with sub-millimetre thickness zirconia substrates. The authors evaluated the stress developed non-linearly as a function of force for a variety of thicknesses. No functional relationship was derived. Similar work is reported by Stolten *et al.* (1995).

B.3 Conclusions

It is clear that there are considerable uncertainties in applying biaxial testing to very thin discs, typically less than 0.5 mm in thickness. The precision with which a linear, small-deflection test can be performed worsens as the size of test-jig declines, so it is not really possible to scale the jig down much beyond, say, a 10 mm diameter support ring. For thin test-pieces of strong materials with strains to fracture above 0.002, the analysis of Kao *et al.* (1971) suggests that:

Non-linear analysis is needed when:

- **the centre deflection to test-piece thickness ratio exceeds about 0.5**
- **the support radius to thickness ratio exceeds about 20**

It is recommended that, as far as possible, the use of non-linear analysis is avoided by appropriate selection of test-piece size and test-jig size relative to the test-piece thickness. This will also reduce the effort required. The fracture stress values computed may be greatly in error if linear analysis is not valid, and any tests would have value only for comparative fracture force purposes. Use of any results for other purposes, such as computation of Weibull statistics or strength prediction purposes could be in serious error. Equation B1 can be used to determine whether a problem might arise.

B.4 Bibliography

Ferriss, D.H. (1991), Large transverse deflections of circular plates loaded symmetrically, NPL Report DMA (A) 86, September 1984.

Ferriss, D.H. (1991), Approximate large deflection analysis of circular plates loaded symmetrically, NPL Report DMM (A) 25, April 1991.

Kao, R.; Perone, N.; Capps, W. (1971), Large deflection solution of the coaxial-ring-circular-glass-plate flexure problem, *J. Amer. Ceram. Soc.*, **54**(11), 566–71.

Kübler, J.; Primas, R.; Gut, B. (1995), Mechanical strength of thermally aged and cycled thin zirconia sheets, *Advances in Science and Technology 3B, Ceramics: Charting the Future*, edited by Vincenzini, P., Techna Srl, Faenza, Italy, pp. 923–8.

Stolten, D.; Monreal, E.; Seesselberg, C. (1995), Testing of SOFC membranes via a biaxial strength and proof-testing device regarding nonlinear structural behaviour, *Advances in Science and Technology 3B, Ceramics: Charting the Future*, edited by Vincenzini, P., Techna Srl, Faenza, Italy, pp. 2613–2620.

Timoshenko, S.P.; Goodier, J.N. (1970), *Theory of elasticity*, 3rd edition, McGraw Hill, New York.

Timoshenko, S.; Woinowsky-Krieger, P (1959), *Theory of plates and shells*, McGraw Hill Book Co., New York, 2nd edition, p72.

Vitman, F.F.; Pukh, V.P. (1963), A method for determining the strength of sheet glass, *Aavodskaya Laboratoriya (Industrial Laboratory)*, **29**, 863–67. (In Russian)

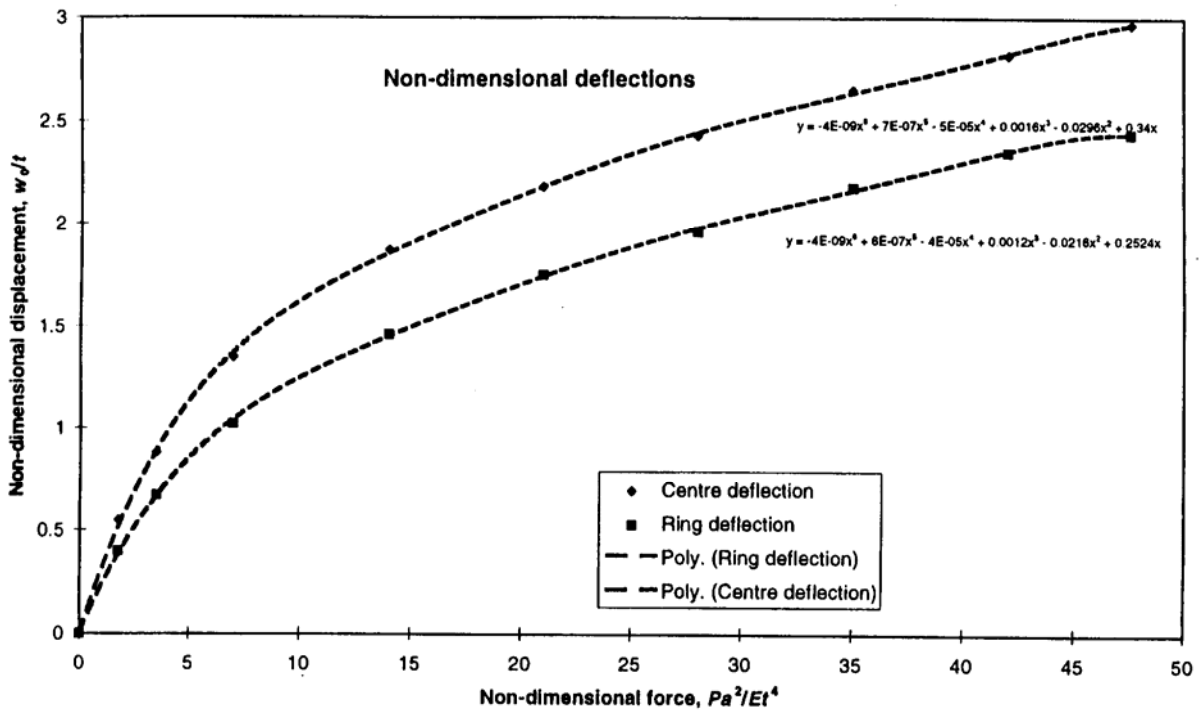


Figure B.1 Thin disc (non-dimensional) central and loading ring deflections as a function of applied (non-dimensional) force for $a/b = 2$ (from Kao et al.(1971)).

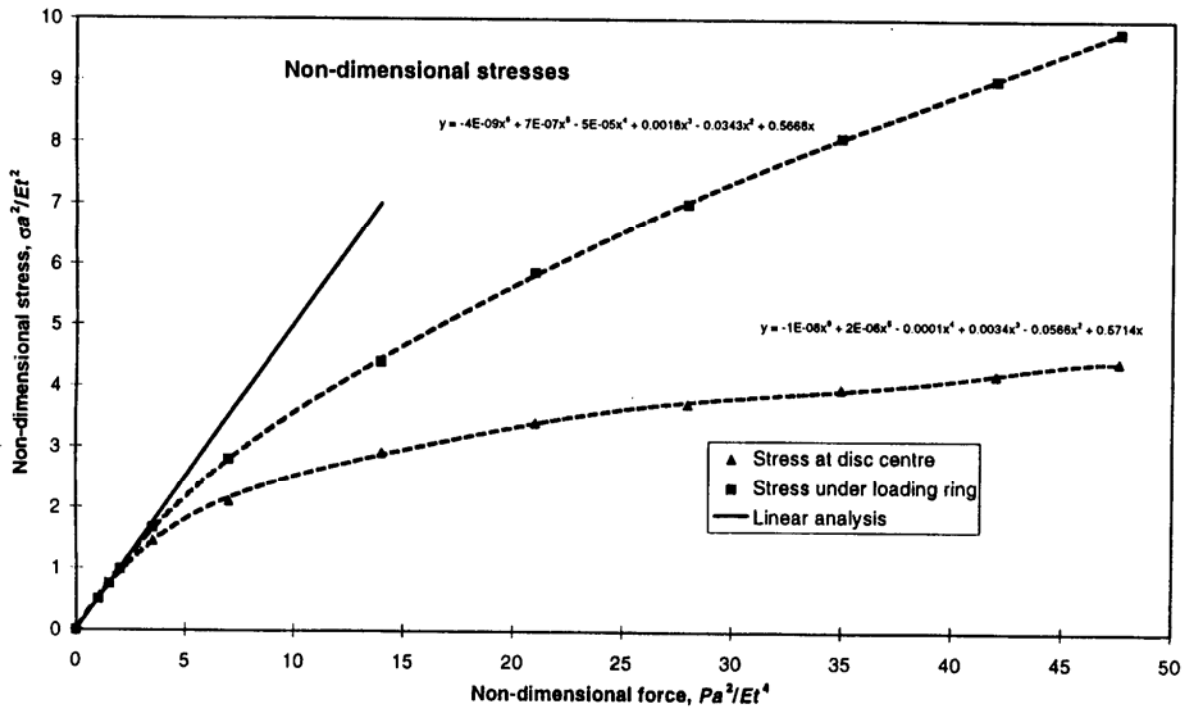


Figure B.2 Thin disc (non-dimensional) stresses at disc centre and under loading ring as a function of non-dimensional force for the case $a/b = 2$ (from Kao et al. (1971)). The straight line is the small-deflection solution.

Annex C – Stress analysis and the role of friction in the ring supported/ring loaded geometry

C.1 Introduction

The basic equations derived for the thin plate, small deflection, ring supported/ring loaded arrangement assume no friction at contacts, and also geometrical perfection. In the beam flexure test, if the contact points are not frictionless, a frictional force exists which opposes the bending moment applied (see NPL Good Practice Guide No. 7). A similar situation arises in biaxial loading of a disc or plate by concentric rings or non-rotating balls. This Annex is concerned with estimating the error involved in ignoring friction. In addition, the use of concentrated forces applied by loading rings leads to non-ideal stresses in the locality of the loading rings. Some of the available information on stress concentration effects is also discussed.

C.2 Stress concentrations

Perhaps the earliest example of detailed analysis is given by Kao *et al.* (1971) in their study of large deformations (see Annex B). Here a small radial tensile stress concentration is found on the tensile side of the test-piece opposite the loading ring, which increases with increasing deflection for large deflections. They demonstrate that its magnitude is also influenced by the relative radii of the loading and support rings. More recently, a number of finite element analyses ignoring friction have been reported in the literature. Ritter *et al.* (1980) give results which appear to show that, in contrast, the tangential stress under the loading ring is enhanced relative to the equibiaxial level experienced within the loading ring diameter, while the radial stress is not. Giovan and Sines (1981) undertook some strain gauging on large-scale test-pieces which showed that opposite the loading ring position, the strain was about 2.5% greater in the tangential direction than in the radial direction, reflecting the well-known stress concentration effects for concentrated loading of beams summarised in Timoshenko and Goodier (1970). These latter results are contradicted by other workers, who find the reverse, in accordance with Kao *et al.*, *e.g.* Adler and Mihora (1992). The magnitude of the concentration depends upon the disc thickness, but is typically several percent. Adler and Mihora show that it also depends on the stiffness of the loading ring relative to the test-piece, and they recommend the use of compliant rectangular section polymer ('Delrin') rings to minimise any effect. A similar analysis has been reported by Morrell *et al.* (1998) for steel rings incorporating the influence of frictional contacts, and is given in the next section.

It is clear from this work that stress concentrations exist, and they can explain the sometimes seen tendency for failures to concentrate around the location of the loading ring. Their magnitude depends on the relative elastic properties of the test material and the loading and support rings, as

well as on the geometry of the test-piece and ring diameters. To minimise the possible errors and permit the accurate application of the thin plate formulae, the use of low modulus materials or load spreaders must clearly be desirable.

C.3 Friction

C.3.1 Analytical approach

Fessler and Fricker (1984) analysed the effects of friction at ring contacts by assuming traction forces proportional to the axial loading forces through a coefficient of friction μ , calculating the bending moment that this produces, and adding the resulting stress field to the simple frictionless solution. In the central region of the disc, they found that the frictionally derived stresses were of magnitude:

$$\Delta\sigma_r, \Delta\sigma_\theta = - \frac{3\mu F}{4\pi t R^2} \left[\frac{2R^2 - (R^2 - b^2)(1-\nu)}{b} + \frac{2R^2 - (R^2 - a^2)(1-\nu)}{a} \right] \quad (\text{C.1})$$

They are negative; in other words they reduce the stress in the central region. To estimate the magnitude of the error, Equation C.1 can be normalised by the frictionless stress (the conventional solution). Figure C.1 shows the fractional central region stress change as a result of friction for two particular cases of $b/a = 0.2$ and 0.5 , with $R = 1.1a$, $\nu = 0.25$, and $\mu = 0.1$. The result scales linearly with friction coefficient, and approximately linearly with increasing thickness to support radius ratio (t/a). It can be seen that for typical discs with t/a of 0.2 , errors incurred in ignoring a friction coefficient of 0.1 only are about 4% , but from equation C.1 clearly increase with increasing μ .

C.3.2 2D finite element analysis (FEA)

A systematic study has been made by Morrell *et al.* (1998) using Rockware Microfield software applied to axisymmetric geometry. Precautions were taken concerning the solutions for the stress fields at critical points, and higher densities of elements were inserted in regions close to the loading and support rings.

A common conclusion of FEA is that there is a small stress concentration on the tensile surface opposite and just inside the loading ring position. The results of this study are shown in Table C.1. For a disc of diameter to thickness ratio of about 40 , the error in ignoring this is small, about 0.2% , but as the disc thickness or the overhang outside the support ring is increased, the error increases, becoming 7% at a diameter to thickness ratio of 6 . The stress at the disc centre also departs from the analytical value for the thicker geometry, being enhanced by 1.6% .

The added effect of friction (equal at support and loading rings) was also estimated for discs with an overhang of 10% of the support diameter, a typical experimental geometry. The effects of friction are more marked than changes in geometry, and cause a reduction in the actual stress over the disc central region compared with the frictionless cases (Figure C.2(a)). The effect is very marked with thicker discs of aspect ratio 6 (Figure C.2(b)). Small stress concentrations still exist near the loading ring which are of similar magnitude to the frictionless case.

Table C.1 – Biaxial flexural strength testing - summary of 2D FEA results

Support ring diam., units [*]	Loading ring diam., units [*]	Disc diam., units [*]	Disc thickness, units [*]	Coeff. of friction	Radial stress error ^{**} relative to analytical solution, %	
					Centre	Near loading ring
2	1	2.02	0.05	0	< -0.1 < -0.1 ^{***}	+0.4 +0.2 ^{***}
2	1	2.1	0.05	0	~ 0	+ 0.5
2	1	2.4	0.05	0 0.2 0.4	~ 0 -1.9 -4.0	+1.1 -0.8 -2.5
2	1	2.4	0.4	0 0.2 0.4	+1.6 -14 -30	+7 -9 -27

* Arbitrary units to provide appropriate aspect ratios

** Hoop stress values are similar to radial stress values at this point

*** Solution with refined mesh in region of support and loading points.

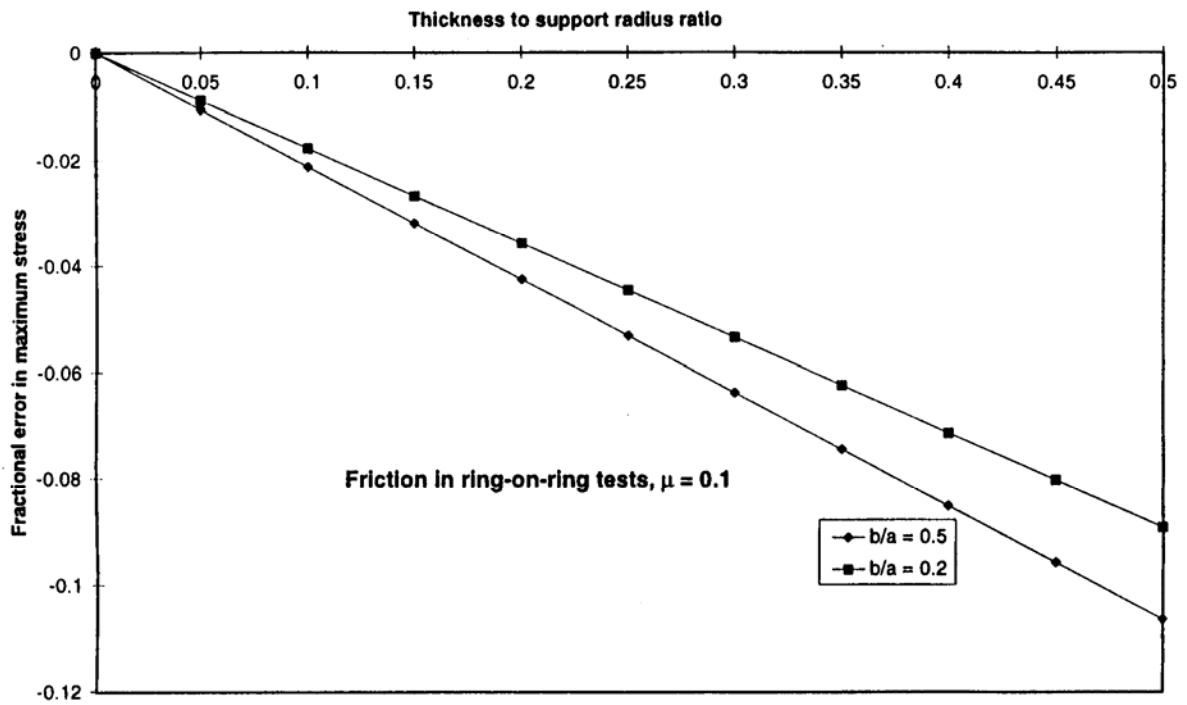


Figure C.1 Analysis of the effects of friction on the nominal central zone equibiaxial stress in the central zone for two ring/ring geometries. The error scales linearly with friction coefficient, after Fessler and Fricker (1984).

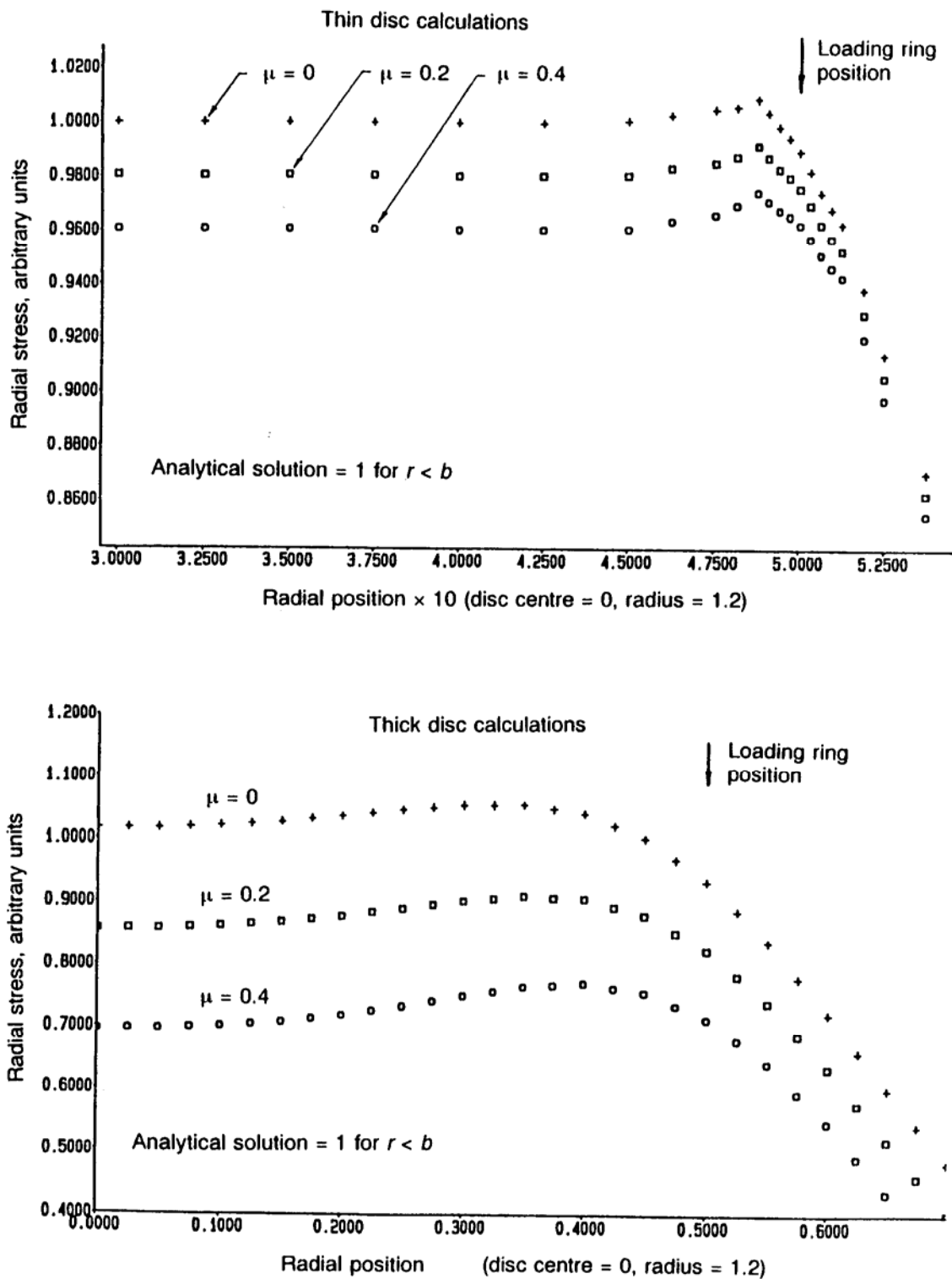


Figure C.2 Radial stress as a function of position for the ring/ring geometry for (a) thin discs ($t/R = 0.042$) and (b) thick disc ($t/R = 0.33$) with increasing friction coefficients.

C.3.3 3D FEA

Morrell *et al.* (1998) also report calculations using an ANSYS 3D FEA package on a Silicon Graphics workstation. The mesh was established basically by devising an in-plane array, and then extruding this in the z-direction. The axisymmetric condition was first examined for disc aspect ratios of 40 and 20 with a 5.6% of disc diameter overhang of the support ring. Uniform normal line forces were applied around the loading and support rings. The calculations proved to be very computer intensive because of the number of elements involved and the need to satisfy the mesh verification tests. No mesh refining techniques were employed because of the complexity of the problem and the need to achieve high precision in the calculations.

For the frictionless condition, the central region radial stress was found to be raised by only 0.5% compared with the analytical solution for the aspect ratio (t/R) of 0.04, and the stress concentration near the loading ring was about 1% (Table C3), figures broadly in line with the 2D axisymmetric results. For boundary conditions in which the no sliding across either the support ring or the loading ring is permitted, which is equivalent to a very high friction coefficient, certainly greater than 1, a significant stress reduction in the central region is produced, in line with the 2D solution, although the reduction is lower for the thicker disc.

Table C3 - Summary of 3D FEA results

Support ring diam., units	Loading ring diam., units	Disc diam., units	Disc thickness, units, friction coeff.	Stress error relative to analytical solution, %	
				Centre	Near loading ring
1.8	0.8	2.0	0.05, $\mu = 0$	~ 0	+ 1.1
			0.05, $\mu \gg 1^*$	- 14	- 12
			0.1, $\mu = 0$	+ 0.5	+ 1.3
			0.1, $\mu \gg 1^*$	- 8	- 4.5

* equivalent to fixed boundary conditions rather than sliding with a given friction coefficient.

C.4 Alignment

There is relatively little information in the literature concerning the magnitude of potential errors due to misalignment of the test piece and/or loading or support rings. Recent work at NPL has shown that maintaining coaxiality, especially of the loading and support rings, is crucial in minimising potential errors. Morrell *et al.* (1998) show an example (Figure C.3) evaluated by 3D FEA where the test-piece and support ring are coaxial, but where the loading ring is displaced by

5% of the support ring radius. This produces a tilt in the radial stress field with typically a 10% rise in the stress opposite the part of the loading ring which is farthest from the support ring. Some attempts have been made to verify this experimentally at NPL, but the results were not conclusive owing to issues of test-piece flatness, finite sizes of strain gauges and difficulties in determining precise positions of alignment. To ensure that alignment errors are less than other errors of calculation, it is recommended that the system be axial to better than 1% of the support ring radius.

The effect of the test-piece not being central compared with the support and loading rings is much less critical. Adler and Mihora (1992) comment that it has little effect on the stress distribution within the loading ring area, and this is reinforced by comments that the precise shape of the test-piece outside the support ring is unimportant (see main text, section 2.5). Tests have been conducted at NPL on large strain-gauged test-pieces which show that other factors such as friction, axiality, and conforming of test-piece and loading rings, are much more critical.

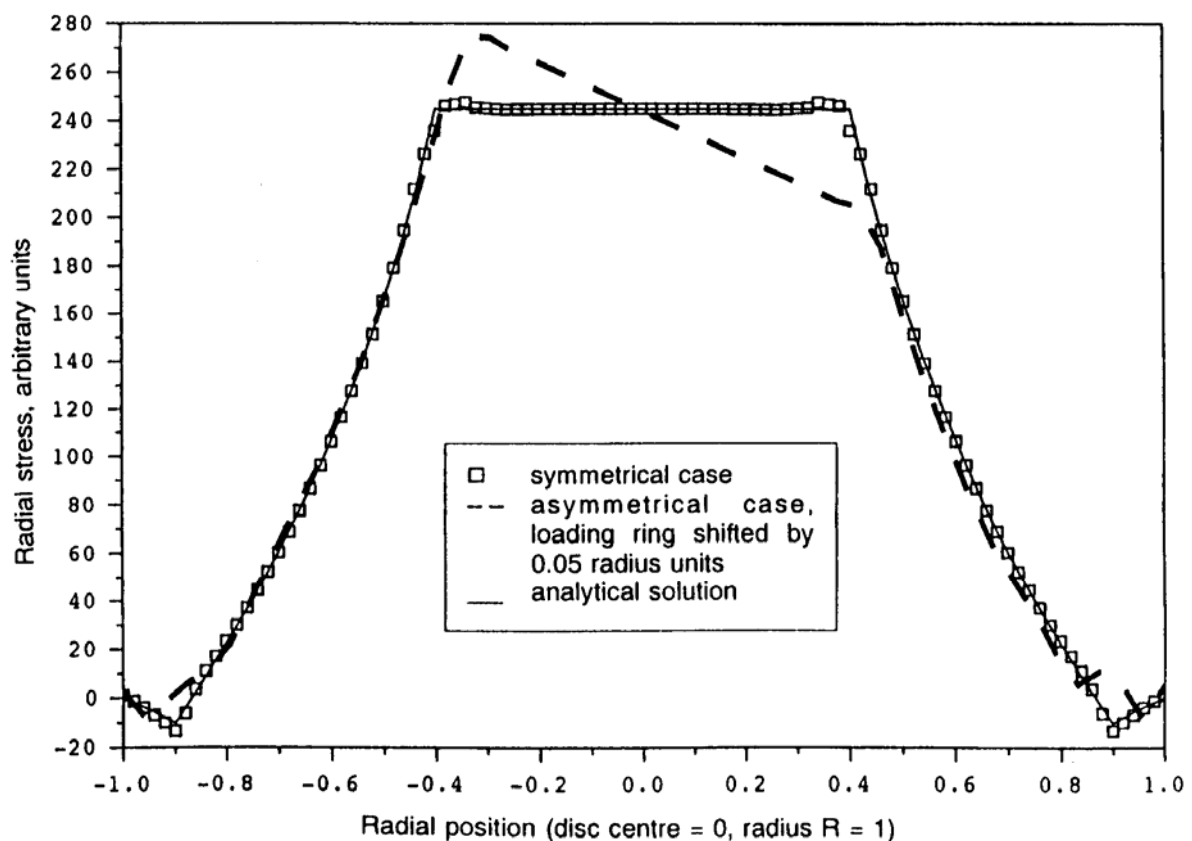


Figure C.3 Effect on radial stress field of lateral shift of the loading ring by 0.05 of the disc radius.

C.5 Bibliography

- Adler, W.F.; Mihora, D.J. (1992), Biaxial flexure testing: analysis and experimental results, *Fracture Mechanics of Ceramics* **10**, edited by Bradt, R.C.; Hasselman, D.P.H.; Munz, D.; Sakai, M.; Shevchenko, V.Ya, Plenum Press, New York, pp. 227-45.
- Fessler, H.; Fricker, D.C. (1984), A theoretical analysis of the ring-on-ring loading disk test, *J. Amer. Ceram. Soc.*, **67**(9), 582–8, Correction: *ibid*, 1988, **71**(10), 904.
- Giovan, M.N.; Sines, G. (1981), Strength of a ceramic at high temperatures under biaxial and uniaxial tension, *J. Amer. Ceram. Soc.*, **64**(2), 68–73.
- Kao, R.; Perone, N.; Capps, W. (1971), Large deflection solution of the coaxial-ring-circular-glass-plate flexure problem, *J. Amer. Ceram. Soc.*, **54**(11), 566–71.
- Morrell, R.; McCormick, N.J.; Bevan, J.; Lodeiro, M.J.; Margetson, J. (1998), Biaxial disc flexure – modulus and strength testing, *IoM Ceramics Convention, April 1998, Royal Agricultural College*, publ. in *Brit Cer. Proc.*, 1999, **59**, 31-44 and *Brit Ceram. Trans.* 1999, **98**(5), 234-40.
- Ritter, J.E., Jr.; Jakus, K.; Batakis, A.; Bandyopadhyay, N. (1980), Appraisal of biaxial strength testing, *J. Non-Cryst. Solids*, **28/9**, 418–29.
- Timoshenko, S.P.; Goodier, J.N. (1970), *Theory of elasticity*, 3rd edition, McGraw Hill, New York.

Annex D – Bibliography on biaxial testing of ceramics and glass

D.1 Introduction

The literature contains a large number of references to the use of biaxial testing on ceramics, either as part of materials evaluation exercises, fractographic investigations, or strength statistical and failure criteria investigations. Some references to this literature not cited elsewhere in this Guide are collected below.

D.2 Bibliography

Amar, E.; Gauthier, F.; Lamon, J. (1989), Reliability analysis of a Si₃N₄ piston pin for automotive engines, *Proc. Conf. Ceramic Materials and Components for Engines*, Las Vegas, Nevada, USA, November 1988, American Ceramic Society, Westerville, Ohio, USA, pp. 1334–46.

Bowles, R. (1973), Strength tests for flat glass samples, *British Glass Industry research Association Technical Note No. 170*.

Chantikul, P.; Lawn, B.R.; Marshall, D.B. (1979), Contact induced failure of pre-stressed glass plates, *J. Amer. Ceram. Soc.*, 62 (7–8), 340–3.

da Costa, C.R.C.; Xavier, C.; Acchar, W. (1988), Comparison between uniaxial and biaxial ring-on-ring tests using an alumina, *Proc. 32nd Brazilian Ceramic Congress, Vol. 1*, Associacao Brasileira de Ceramica, San Paulo, Brasil, pp. 365–79. (In Portuguese)

Cunha, P.A.; Neto, F.P.; Cairo, C.A.A.; De Melo, F.C.L.; Devezas, T. (1987), Correlation between uniaxial and biaxial tests for evaluation of mechanical properties of advanced ceramics, *Ceramica (Sao Paulo)*, 33(210), 159–62. (In Portuguese)

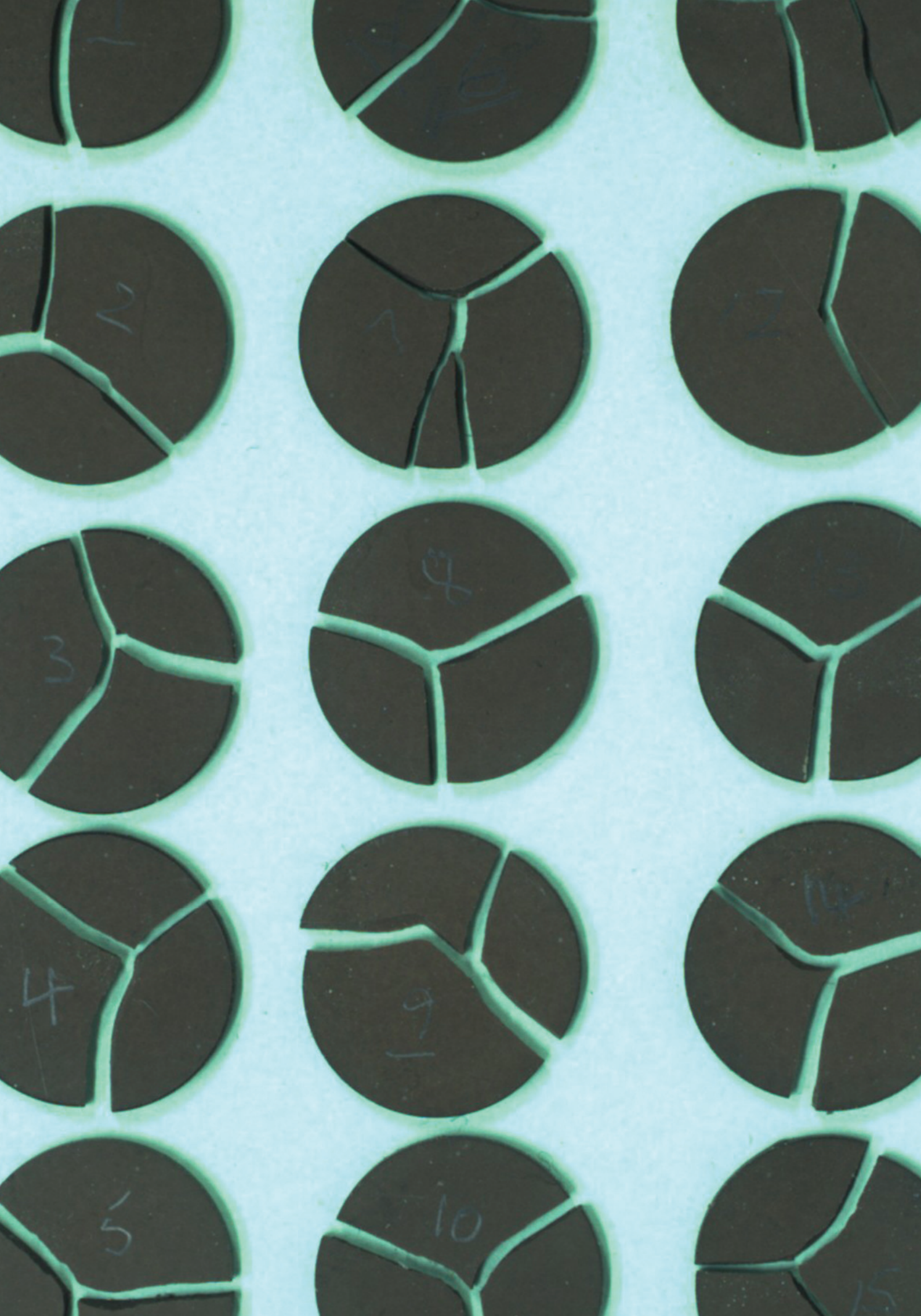
Donald, I.W.; Hill, M.J.C. (1988), Preparation and mechanical behaviour of some chemically strengthened lithium magnesium alumino-silicate glasses, *J. Mater. Sci.*, 23, 2797–2809.

Giovan, M.N.; Sines, G. (1979), Biaxial and uniaxial data for statistical comparisons of a ceramic's strength, *J. Amer. Ceram. Soc.*, 62(9–10), 510–5.

Glandus, J.C.; Boch, P. (1980), Use of disc-shaped specimens for measuring the mechanical properties of brittle materials, *Mém. Sci. Rev. Métall.*, 77(1), 27–32. (In French)

- Gruniger, M.F.; Wachtman, J.B., Jr.; Haber, R.A. (1987). Thermal shock protection of dense alumina substrates by porous alumina sol-gel coatings, *Cer. Eng. Sci. Proc.*, **8**(7–8), 596–601.
- Ham-Su, R., Wilkinson, D.S. (1995), Strength of tape cast and laminated ceramics, *J. Amer. Ceram. Soc.*, **78**(6), 1580–4.
- McMahon, G.; Wang, S.S.B.; Quon, D.H.H.; Sood, R.R.; Holt, R.T.; Maccagno, T.M. (1989), A study on whisker reinforced lithium aluminosilicate composites, *Proc. Int. Symp. Advanced Structural Materials, 28–31 Aug. 1988, Montreal, Canada*, Pergamon Press, New York, USA, pp. 179–186.
- Mecholsky, J.J., Jr.; Rice, R.W. (1982), Fractographic analysis of biaxial failure in ceramics, in *Fractography of ceramic and metal failures*, ASTM STP 827, ASTM, Philadelphia, PA, USA, pp. 185–93.
- Nakasuji, Y.; Yamada, N.; Tsuruta, H.; Masuda, M.; Matsui, M. (1992), Fracture behaviour of non-oxide ceramics under biaxial stresses, *Fracture Mechanics of Ceramics 10*, edited by Bradt, R.C.; Hasselman, D.P.H.; Munz, D.; Sakai, M.; Shevchenko, V.Ya, Plenum press, New York, pp. 211–226.
- Okada, A.; Kawamoto, H.; Usami, H. (1997), Microstrength evaluation of alumina using biaxial flexure technique, *Cer. Eng. Sci. Proc.*, **18**(4), 183–90.
- Ovri, J.E.; Davies, T.J. (1987), Uniaxial and biaxial strengths of a sintered ferrite, *Science of ceramics*, **14**, 199–605
- Radford, K.C.; Lange, F.F. (1978), Loading (L) factors for the biaxial test, *J. Amer. Ceram. Soc.*, **61**(5–6), 211–3.
- Scholten, H.F.; Dortmans, L.J.; de With, G. (1993), Application of mixed-mode fracture criteria for weakest-link failure prediction for ceramic materials, in *Life Prediction Methodologies and Data for Ceramic Materials*, Cocoa Beach, Florida, USA, Jan. 1993, ASTM STP 1201, pp. 192–206.
- Shetty, D.K.; Rosenfield, A.R.; Duckworth, W.H.; Held, R.R. (1983), A biaxial-flexure test for evaluating ceramic strengths, *J. Amer. Ceram. Soc.*, **66**(1), 36–42.
- Tanatar, B.; Canessa, E. (1992). Pattern formation in concentrically loaded square plates, *J. Mater. Sci. Lett.*, **11**, 401–3.

Thiemeier, T.; Brückner-Foît, A.; Koelker, H. (1991), Influence of the fracture criterion on the failure prediction of ceramics loaded in biaxial flexure, *J. Amer. Ceram. Soc.*, **74**(1) 48–52.



1

2

3

4

5

6

7

8

9

10

11

12

13

14

15